Arabidopsis lines with modified ascorbate concentrations reveal a link between ascorbate and auxin biosynthesis

Fenech M.[1,3]*, Zulian V.[2], Moya-Cuevas J.[3,4], Arnaud D.[5], Morilla I.[6,7], Smirnoff N.[5], Botella M.A.[3], Stepanova A.N.[1], Alonso J.M.[1], Martin-Pizarro C.[3], Amorim-Silva V.[3]*

*Corresponding authors. MF: mfenech2@ncsu.edu/mfenechtorres@gmail.com, VAS: vitoramorimsilva@uma.es

[1] Department of Plant and Microbial Biology, College of Agriculture and Life Sciences, North Carolina State University, 112 Derieux Place, Raleigh, North Carolina 27695-7614, United States of America

[2] Department of Biological Sciences, Clemson University, 132 Long Hall, Clemson, South Carolina 29631, United States of America

[3] Área de Mejora y Fisiología de Plantas, Instituto de Hortofruticultura Subtropical y Mediterránea "La Mayora", Universidad de Málaga-Consejo Superior de Investigaciones Científicas (IHSM-UMA-CSIC), Universidad de Málaga, Campus Teatinos, 29010, Málaga, Spain

[4] Current affiliation: Foundation for Research and Technology Hellas, IMBB/FORTH, Institute of Molecular Biology and Biotechnology, N Plastira Str 100, Irakleio, 70013, Greece

[5] Biosciences, Faculty of Life and Environmental Sciences, University of Exeter, Exeter, EX4 4QD, UK

[6] Área de Protección de Cultivos, MLiMO, Instituto de Hortofruticultura Subtropical y Mediterránea "La Mayora", Universidad de Málaga-Consejo Superior de Investigaciones Científicas (IHSM-UMA-CSIC), Universidad de Málaga, Campus Teatinos, 29010, Málaga, Spain

[7] Université Sorbonne Paris Nord, LAGA, CNRS, UMR 7539, F-93430, Villetaneuse, France

Short title: Ascorbate concentration alters auxin homeostasis.

The authors responsible for distribution of materials integral to the findings presented in this article in accordance with the policy described in the Instructions for Authors (https://academic.oup.com/plphys/pages/General-Instructions) are MF and VAS.

Abstract

Ascorbate is the most abundant water-soluble antioxidant in plants and an essential molecule for normal plant development. Although present in all green plants, ascorbate concentrations vary among plant species and tissues. While ascorbate accumulation is a trait of nutritional, and therefore, agronomical interest, the impact of different concentrations on cellular homeostasis remains elusive. To shed light on this question, we compared Arabidopsis (*Arabidopsis thaliana*) lines with very low (*vtc2* mutant, 20% of wild-type (WT) levels), low (*vtc4* mutant, 65% of WT levels), and high (*vtc2/OE-VTC2*, 165% of WT levels) ascorbate concentration in four-week-old rosette leaves. An 80% reduction of ascorbate increased the expression of genes implicated in defense against pathogens but repressed genes associated with abiotic stress responses. Unexpectedly, lines with increased (165% of WT) and decreased (65% of WT) ascorbate levels shared 85% of induced transcription factors and the gene ontology terms associated with their transcriptional programs. We identified *TRYPTOPHAN AMINOTRANSFERASE OF ARABIDOPSIS 1 (TAA1)*, a gene encoding the enzyme that catalyzes the first step of auxin biosynthesis, among the group of genes whose expression was positively correlated with ascorbate content. Using a combination of genetic and pharmacological approaches in fluorescent and histochemical reporter lines for auxin biosynthesis and signaling activity, we revealed that TAA1- and TAA1 RELATED 2 (TAR2)-mediated auxin biosynthesis is necessary for plants to cope with increased ascorbate concentration in a light-dependent manner, revealing a layer of complexity in the regulatory landscape of redox homeostasis.

Introduction

L-Ascorbate (ascorbate), also known as vitamin C, is the most abundant water-soluble antioxidant in plants. Humans, among other groups of animals, have lost the ability to synthesize ascorbate throughout evolution due to a lack of selective pressure as fruits and vegetables became a substantial part of our diet (Chatterjee, 1973; Smirnoff, 2018). Ascorbate deficiency in humans leads to scurvy, a disease considered rare although there are still numerous cases in modern society due to an increasing trend in choosing fast food (Lipner, 2018; Urueña-Palacio et al., 2018), with pediatric cases increasing by three-fold in the period 2016-2020 (Reikersdorfer et al., 2024). In addition to preventing scurvy, ascorbate is involved in many other processes in humans as a cofactor in various biological processes and it plays a major role in gene expression regulation (Blaschke et al., 2013; Minor et al., 2013; Hu et al., 2015; Young et al., 2015; Padayatty and Levine, 2016). The abovementioned reports suggest that in humans, ascorbate is not only critical for maintaining cell redox state but also for epigenetic regulation of gene expression and chromatin remodeling. Because the major source of vitamin C in humans is fresh produce, understanding how plants

biosynthesize ascorbate, and how altered concentrations of this antioxidant impact plant development, is critical.

In plants, ascorbate is also a crucial molecule for normal development, with ascorbate-deprived mutants showing lethality that can be rescued by exogenous supplementation with ascorbate (Dowdle et al., 2007; Pineau et al., 2008; Lim et al., 2016; Fenech et al., 2021). Among its numerous roles described in plants, ascorbate is required to maintain the oxidative status in the active center of several enzymes like the Cu^{2+} and Fe^{2+}/α-ketoglutarate-dependent dioxygenases —for example, 4-hydroxyphenylpyruvate dioxygenase involved in plastoquinone and tocopherol biosynthesis (Norris et al., 1998)—, modulating redox-sensitive processes such as anthocyanin biosynthesis (Page et al., 2012), as well as to scavenge reactive oxygen species (ROS) produced during photosynthesis (Tyystjärvi, 2008; Tóth et al., 2013), normal plant development (Wu et al., 2023), or in response to pathogens (Barth et al., 2004; Pavet et al., 2005; Mukherjee et al., 2010).

The rate-limiting step of ascorbate biosynthesis in plants is catalyzed by GDP-L-galactose phosphorylase (GGP), which is encoded by *VITAMIN C DEFICIENT 2* (*VTC2)* and *VTC5* in Arabidopsis (Fig. 1A) (Dowdle et al., 2007; Linster et al., 2007; Bulley et al., 2009; Fenech et al., 2021). The translation of *GGP* mRNA is controlled by an upstream open reading frame (uORF), which is proposed to mediate feedback repression by ascorbate (Laing et al., 2015; Baldet et al., 2024). *GGP* expression is controlled transcriptionally by light (Dowdle et al., 2007) and its activity is reversibly inhibited by a Per-ARNT-Sim/Light-Oxygen-Voltage (PAS/LOV) protein (PLP) photoreceptor when exposed to blue light in Arabidopsis (Aarabi et al., 2023) and tomato (Bournonville et al., 2023), thus linking light signaling and ascorbate production.

Ascorbate concentration is typically higher in leaves and lower in roots, with some species having exceptionally high levels in their fruits (Fenech et al., 2019). In wild-type (WT) Arabidopsis leaves, ascorbate concentration usually ranges from 2 to 5 μmol g^{-1} fresh weight (FW) under low to moderate light intensities, which is comparable to the concentrations of the most prevalent primary metabolites such as sucrose, glucose, serine, and glutamate (Szecowka et al., 2013). However, Arabidopsis *vtc2* mutants with reduced ascorbate levels (~20% of the WT) remain viable with near to normal growth under benign conditions (Lim et al., 2016). However, ascorbate deficiency results in increased sensitivity to some abiotic stresses and activation of basal pathogen defenses (Barth et al., 2004; Pavet et al., 2005; Mukherjee et al., 2010; Arnaud et al., 2022; Smirnoff and Wheeler, 2024).

Ascorbate has also been implicated in the crosstalk with other regulatory molecules, such as phytohormones, to help tune signaling cascades in response to various stresses (Akram

et al., 2017; Veljović-Jovanović et al., 2017). Specifically, ethylene and ABA regulate ascorbate biosynthesis by controlling VTC2 expression through ETHYLENE INSENSITIVE 3 (EIN3) (positive regulator of VTC2 expression) and ABA INSENSITIVE 4 (ABI4) (negative regulator) to tune ascorbate concentration and, therefore, ROS levels (Yu et al., 2019). Reciprocally, altered ascorbate status has been reported to influence salicylic acid, jasmonic acid, and abscisic acid (ABA) concentrations (Pastori et al., 2003; Bulley et al., 2009). Additionally, early reports suggested that auxin—a master regulator of plant growth and development (Zhao, 2018)—may also interact with ascorbate by means of ASCORBATE PEROXIDASE (APX)-mediated indole-3-acetic acid (IAA) decarboxylation and maintenance of the root quiescent center (Kerk et al., 2000; Jiang et al., 2003).

IAA—the major active form of auxin in plants—is biosynthesized from the amino acid tryptophan (Trp) in two steps by two multi-gene families. First, Trp is converted into indole-3-pyruvic acid (IPyA) by a tryptophan aminotransferase encoded by three genes in *Arabidopsis thaliana* (hereon, Arabidopsis): *TRYPTOPHAN AMINOTRANSFERASE OF ARABIDOPSIS 1 (TAA1)*, *TAA1 RELATED 1* (*TAR1)*, and *TAR2* (Stepanova et al., 2008; Tao et al., 2008; Yamada et al., 2009). Then, a family of flavin monooxygenases, represented in Arabidopsis by *YUCCA 1 (YUC1)* through *YUC11*, catalyzes the conversion of IPyA into IAA (Zhao et al., 2001; Stepanova et al., 2011). The spatiotemporal regulation of local auxin biosynthesis and the auxin transport patterns confer the very finely-tuned control of auxin activity (Brumos et al., 2018; Brumos et al., 2020) that governs fundamental physiological responses like shade avoidance (Tao et al., 2008), phototropism (Liscum et al., 2014), root gravitropism (Bennett et al., 1996; Marchant et al., 1999), and root cell identity and architecture (Delarue et al., 1998; Zhao et al., 2001; Marchant et al., 2002; Stepanova et al., 2008; Lavenus et al., 2013; Roychoudhry and Kepinski, 2022). Consistent with a potential interaction between ascorbate and auxin signaling pathway, ascorbate has also been reported to alter root gravitropism (Joo et al., 2001; Lee et al., 2011) or root cell identity (Lee et al., 2007).

An interaction between auxin and ascorbate is further supported not only by the abovementioned studies but also by the antagonistic effects of auxin (Mangano et al., 2017) and ascorbate (Tyburski et al., 2012) on ROS-mediated cell elongation of root hairs. While auxin induces *ROOT HAIR DEFECTIVE 6-LIKE 4 (RSL4)*-mediated ROS production and root hair elongation (Mangano et al., 2017), high concentrations of ascorbate lead to shorter root hairs (Tyburski et al., 2012). Reciprocally, ROS concentration also regulates auxin distribution (Pasternak et al., 2023), which provides a mechanistic insight on how ascorbate and other antioxidants may disrupt root gravitropism (Joo et al., 2001). Given the well-established role of ascorbate as a ROS scavenger (Foyer and Kunert, 2024), the antagonistic roles of IAA and ascorbate are thought to stem from their opposite effects on ROS production

and neutralization (Wang et al., 2021). Accordingly, ascorbate biosynthesis must be finely tuned to ensure the right spatiotemporal distribution of ROS and normal plant development.

To shed light on ascorbate's mechanism of action, we performed a transcriptomic study that leveraged Arabidopsis plants with reduced and elevated ascorbate levels caused by altered expression of *VTC2* and *VTC4*. GGP (VTC2/VTC5) is the first step in the pathway that does not produce cell wall precursors (Fig. 1A). Consistently, ascorbate biosynthesis mutants affected in steps upstream of GGP have cell wall and growth defects or even lethality at the gametophyte (Mounet-Gilbert et al., 2016; Qi et al., 2017) or embryo (Lukowitz et al., 2001) stages, while *ggp* and downstream mutants lethality can be prevented by exogenous supplementation of ascorbate (Dowdle et al., 2007; Pineau et al., 2008; Fenech et al., 2021). Previous transcriptomic work in Arabidopsis used *vtc2-1* (Kerchev et al., 2011), which carries additional mutations causing small size (Lim et al., 2016) or *vtc1* that also affects the biosynthesis of cell wall precursors (Pastori et al., 2003) and protein N-glycosilation (Qin et al., 2008). Consequently, the transcriptional changes observed reflected both the altered concentration of endogenous ascorbate and structural impairment due to defective growth and cell walls (Lukowitz et al., 2001; Kerchev et al., 2011), making it difficult to disentangle the effects of these two factors. In contrast, the germplasm we chose for our study primarily affects ascorbate biosynthesis. We identified a set of genes whose expression levels correlate with ascorbate concentration and investigated whether a specific transcription factor or subset of transcription factors could regulate gene expression in response to changes in ascorbate levels. In this study, we did not identify specific TFs that correlate with the ascorbate concentration, supporting the notion of complex transcriptional regulation of ascorbate homeostasis in plants, and we characterized the importance of the phytohormone auxin in response to increased ascorbate concentration.

Results

The endogenous levels of ascorbate do not exert major control over the expression of genes involved in ascorbate homeostasis

To investigate how different levels of ascorbate affect gene expression, we used Arabidopsis lines with reduced and increased endogenous concentrations of ascorbate relative to WT. We selected knockout mutant lines of *VTC2*, defective in GGP (*vtc2-4*, from now on *vtc2*; Lim et al., 2016), and of *VTC4,* disrupted in the *L-GALACTOSE 1-PHOSPHATE PHOSPHATASE* (*GPP*) gene (*vtc4-4,* from now on *vtc4*; Torabinejad et al., 2009) (Fig. 1A). We chose these two mutants because *VTC2* and *VTC4* are specifically involved in ascorbate biosynthesis and not in cell wall biosynthesis (Fenech et al., 2019). To obtain lines with elevated ascorbate content, we generated transgenic plants in the *vtc2* background expressing the *VTC2* coding

DNA sequence (CDS) lacking the repressive upstream open reading frame (uORF) and fused to *GREEN FLUORESCENCET PROTEIN (GFP)* under the control of the cauliflower mosaic virus (CaMV) *35S* promoter. We have previously shown that *VTC2* is the only gene of the pathway that, upon overexpression, increases ascorbate content (Fenech et al., 2021). Two *vtc2/35S: VTC2$_{CDS}$-GFP* lines were selected, *vtc2/OE-VTC2 L15* and *L16,* that showed higher amounts of VTC2-GFP protein compared with the *vtc2* mutant complemented with the *VTC2p:VTC2$_{CDS}$-GFP* construct driven by the *VTC2* promoter and harboring the repressive uORF (Fenech et al., 2021) (Fig. 1B). For further studies we selected line *L15* (from now on, *vtc2/OE-VTC2*) because it accumulated a higher amount of the VTC2-GFP protein than *L16* (Fig. 1B).

The ascorbate concentration in WT was 3.2 mol g^{-1} FW, while the concentrations for *vtc2, vtc4*, and *vtc2/OE-VTC2* were approximately 20%, 65%, and 165% of WT levels, respectively, indicating a progressive increase in ascorbate concentration among these lines (*vtc2* < *vtc4* < WT < *vtc2/OE-VTC2*) (Fig. 1C). To determine how this range of endogenous ascorbate concentration affects gene expression, we conducted RNA-seq on the same four-week-old WT, *vtc2*, *vtc4*, and *vtc2/OE-VTC2* rosettes from which ascorbate concentration was determined (gene expression and ascorbate concentration are available in Supplementary Dataset S1). As expected, we found very low expressions of *VTC2* and *VTC4* in their respective mutants (Fig. 1D). Interestingly, altered levels of endogenous ascorbate had very little effect on the expression of genes involved in the mannose/L-galactose ascorbate biosynthesis pathway (Fig. 1D), metabolism, and regulation (Supplementary Figs. S1 and S2). Notably, although the *VTC2* mRNA levels in the CaMV*35S* lines (*vtc2/OE-VTC2*) were lower than in WT (Fig. 1D), protein accumulation was much higher than that in line *vtc2/VTC2p:VTC2$_{CDS}$-GFP* where *VTC2* is expressed by its own promoter and its translation is regulated by the uORF within its native 5' untranslated region (5' UTR)(Fenech et al., 2021) (Fig. 1B). The elevated VTC2 protein levels in *vtc2/OE-VTC2* lines lacking its regulatory uORF are consistent with the inhibitory role of that uORF on the translation of *VTC2* (Laing et al., 2015).

Comparative analysis of plants with altered ascorbate content unexpectedly reveals common differentially expressed genes between lines with contrasting levels of ascorbate

We investigated the transcriptional changes in the three Arabidopsis lines with different endogenous ascorbate concentrations (*vtc2, vtc4* and *vtc2/OE-VTC2*) compared with WT. To determine differentially expressed genes (DEGs), we used a false discovery rate (FDR)-corrected *p*-value (*q*-value) <0.05 (Supplementary Dataset S2). The number of DEGs in the three lines compared to WT (Fig. 2A) and the profile of their volcano plots (Supplementary

Fig. S3A) showed a greater difference in the *vtc2* transcriptional program compared to the other lines, supported by the sample outgrouping within the principal component analysis (PCA) plot (Supplementary Fig. S3B). A total of 786 DEGs were found in *vtc2* (506 upregulated and 280 downregulated), 147 DEGs in *vtc4* (123 up and 24 down) and 164 DEGs in *vtc2/OE-VTC2* (135 up and 29 down) (Fig. 2A). These differences in the number of DEGs between *vtc2* and those of *vtc4* and the overexpression line are likely the result of the large difference in ascorbate concentration among these lines (Fig. 1C). We found that ascorbate-deficient mutants *vtc2* and *vtc4* had in common 35 induced genes and 12 repressed genes (Fig. 2B and Supplementary Fig. S4A and B). This non-random overlap (α=0.05, *p*-values of 3.07×10^{-34} and 3.12×10^{-19} for induced and repressed genes, respectively) was expected since both *vtc2* and *vtc4* have reduced ascorbate levels (Fig. 1C; Supplementary Fig. S4B). Unexpectedly, however, a comparison of DEGs between *vtc4* and *vtc2/OE-VTC2*, the two lines that have reduced or elevated ascorbate content, respectively, shared 82 induced genes (*p*-value=5.28×10^{-177}) and 4 repressed genes (*p*-value=5.36×10^{-9}) (Fig. 2B; Supplementary Fig. S4A and B).

To investigate the overlap and differences of their transcriptional programs, we determined the processes impacted by altered ascorbate levels by analyzing the Biological Process Gene Ontology (GO) terms enriched in the induced and repressed DEGs (Fig. 2C and D). The most enriched GO terms for induced DEGs in *vtc2*, but not in *vtc4*, are related to biotic stress, consistent with previous reports where very low ascorbate increased the expression of salicylic acid-responsive genes leading to the higher basal disease resistance of *vtc* mutants (Mukherjee et al., 2010; Kerchev et al., 2011; Pastor et al., 2013) (Fig. 2C). On the other hand, the GO terms enriched for genes repressed in both *vtc2* and *vtc4* partially overlapped for broader terms such as response to stimulus and response to abiotic stress, although *vtc2*-repressed GOs were enriched in abiotic stress and *vtc4´*s in biotic stress (Fig. 2D). Consistent with the overlap between *vtc4*- and *vtc2/OE-VTC2*-induced DEGs, similar enriched GO terms such as homologous recombination, DNA recombination, and organelle organization were identified (Fig. 2C). The reason why both an increase (*vtc2/OE-VTC2*) and a decrease (*vtc4*) of ascorbate concentrations caused a subset of DEGs and GOs terms to respond similarly remains unknown, but it could be the result of an oxidative imbalance of the cell.

Transcription factors associated with differences between transcriptional programs

We used TDTHub (Grau and Franco-Zorrilla, 2022) and Plant Regulomics (Ran et al., 2020) databases to identify enrichments in DNA motifs and transcription factor (TF) binding sites (TFBSs) within the induced and repressed genes (Supplementary Dataset S3). The analysis of *vtc2*'s repressed and induced genes revealed a significant enrichment of putative targets

from the basic leucine zipper (bZIP) family, like ABA INSENSITIVE 5 (ABI5), and from the WRKY family, respectively, with an FDR<0.05. Among the top ten most enriched TFBS within the promoters of *vtc2*-induced genes, with all of them being the putative targets of WRKY family, we found the recognition sequences of WRKY70, WRKY30, WRKY47, and WRKY55, and these TFs happen to be transcriptionally induced in *vtc2*. The lists of enriched TFBSs in induced DEGs overlapped between *vtc4* and *vtc2/OE-VTC2* but differed from that in *vtc2*. Specifically, *SQUAMOSA PROMOTER BINDING PROTEIN-LIKE 3* (*SPL3/AT2G33810)* and *MYB DOMAIN PROTEIN 116* (*MYB116/AT1G25340)* target sites were enriched among both *vtc4*- and *vtc2/OE-VTC2*-induced genes (Supplementary Dataset S3). For the repressed genes, HOMEOBOX (*AtHB*) TFBSs were enriched among *vtc2/OE-VTC2*-downregulated genes, but no enrichment was found within *vtc4*-downregulated genes by either TDTHub or Plant Regulomics.

To identify DEGs encoding transcriptional regulators (TRs), i.e., TFs and other regulators not binding DNA, that may account for the differences in the transcriptomic profiles of the different ascorbate lines, we used the list of manually curated Arabidopsis TRs obtained from AGRIS (Davuluri et al., 2003; Palaniswamy et al., 2006; Yilmaz et al., 2011; Spurney et al., 2020) (Supplementary Dataset S4). A total of 50 TR genes (28 upregulated, 22 downregulated) were identified among *vtc2*-dependent DEGs, while 7 and 8 TRs were identified among *vtc4*- and *vtc2/OE-VTC2*-controlled DEGs, respectively, with all of them induced. Remarkably, the *vtc4*- and *vtc2/OE-VTC2*-regulated TR gene lists shared 6 upregulated genes, including *SHOOT MERISTEMLESS* (*STM*) involved in the maintenance of shoot and flower meristem (Endrizzi et al., 1996) (Fig. 2E). Interestingly, all lines shared one differentially expressed TR gene, *GROWTH REGULATING FACTOR 1 (GRF1)-INTERACTING FACTOR 1/ANGUSTIFOLIA 3* (*GIF1/AN3/AT5G28640*), which coordinates leaf meristem positioning, cell proliferation, and postmitotic cell expansion in leaves (Kawade et al., 2010) (Fig. 2E). Notably, among the TRs upregulated in *vtc2*, 18 out of 28 genes belong to the *WRKY* (10 genes) and *NO APICAL MERISTEM/ARABIDOPSIS TRANSCRIPTION ACTIVATION FACTOR/CUP-SHAPED COTYLEDON* (*NAC*) (8 genes) families (Fig. 2E), with many of them implicated in the response to biotic stress, crosstalk with ROS, hormone signaling, and leaf senescence (Chen et al., 2019; Yuan et al., 2019; Bian et al., 2020; Ahmad et al., 2024). In contrast, some *ETHYLENE RESPONSE FACTOR* (*ERF*) genes like *ERF018/ACTIVATOR PROTEIN BINDING TO CMSRE-1 3 (ACRE3), ERF094/ OCTADECANOID-RESPONSIVE AP2/ERF 59 (ORA59),* and *ERF023* were among the most-repressed TR genes in *vtc2* (Supplementary Dataset S4). In addition, TRs associated with shade avoidance response and response to nitrogen concentration by modulating cytokinin (*BRASSINOSTEROID-ENHANCED EXPRESSION 1* (*BEE1)* (Gautrat et al., 2024) and *CYTOKININ RESPONSE FACTOR 2* (*CRF2)* (Chen et al., 2024)) and auxin (*IAA6/SHORT HYPOCOTYL 1* (*IAA6/SHY1)*

(Kim et al., 1996; Nguyen et al., 2023) and *IAA17/AUXIN RESISTANT 3* (*IAA17/AXR3*) (Leyser et al., 1996)) signaling pathways were also repressed in *vtc2*. These results suggest an interplay between ascorbate and hormone signaling.

Refining the regulatory landscape of ascorbate-correlated genes

Variations in ascorbate concentration across the four genotypes analyzed enabled the identification of genes whose expression correlated with endogenous ascorbate levels. Using Pearson correlation analysis with an FDR-corrected p-value threshold (q-value<0.05), we identified 474 positively correlated genes (PCGs) and 376 negatively correlated genes (NCGs) (Supplementary Dataset S5). Further filtering based on differential expression between *vtc2* and *vtc2/OE-VTC2* (t-test, q-value<0.05) narrowed this down to 90 PCGs and 107 NCGs whose expression in *vtc2* is complemented by *vtc2/OE-VTC2* (Fig. 3A and B; Supplementary Dataset S6A and B). The expression patterns of these genes visually confirmed their correlation with ascorbate concentration (Fig. 3C and D).

To better characterize their response to varying ascorbate levels, we examined expression fold changes in samples with the most contrasting ascorbate concentrations—*vtc2* (low ascorbate) and *vtc2/OE-VTC2* (high ascorbate) (Supplementary Fig. S5A and B). Genes were classified into three categories: (i) those responsive to ascorbate depletion (44 PCGs, 57 NCGs), (ii) those responsive to ascorbate excess (25 PCGs, 35 NCGs), and (iii) those exhibiting a proportional response to ascorbate levels (expected response; 21 PCGs, 15 NCGs). To quantify their relative response, we assessed the fold-change distance from the origin (0,0) in Supplementary Fig. S5A and B, normalized against a theoretical 1:1 response between fold change in gene expression and ascorbate levels (Supplementary Fig. S6A and B). PCGs primarily showed mild responses (12.5-37.5% of an ideal PCG), with only one gene surpassing 50%. In contrast, a greater proportion of NCGs exceeded 50%, with some reaching ~80% (Supplementary Fig. S6C). These findings suggest that transcriptional changes due to ascorbate fluctuations may be mediated by additional factors such as reactive oxygen species (ROS) or other signaling molecules.

Transcriptional Regulation of Ascorbate-Correlated Genes

To investigate whether ascorbate-correlated genes are co-regulated by specific transcription factors (TFs), we leveraged the DAP-seq dataset (O'Malley et al., 2016). We focused on TFs targeting the promoters of PCGs and NCGs responding proportionally to ascorbate levels. Hierarchical clustering of PCG and NCG based on the TF that they are targeted by, and spatially arranged based on their relative response (using their FC *vtc2*), allowed us to identify distinct TF subsets (Supplementary Fig. S5C and D; Supplementary

Dataset S7). Among PCGs, circadian clock-associated TFs, including REVEILLE 4 (RVE4), RVE8, and LATE ELONGATED HYPOCOTYL (LHY), as well as ERFs were prominent (Supplementary Fig. S5C; Supplementary Dataset S7A). In contrast, NCGs were primarily targeted by WRKY TFs such as WRKY18, WRKY33, and WRKY40, known for their roles in biotic stress responses (Liu et al., 2015; Birkenbihl et al., 2017) (Supplementary Fig. S5D; Supplementary Dataset S7B). Remarkably, these TFs were not specifically targeting the "responding as expected" class of NCGs, and many other correlated genes were also targeted by WRKYs (Supplementary Dataset S8), suggesting that they may play a broader role in ascorbate-mediated transcriptional regulation. To further explore the possibility that a subset of TF could regulate the expression of ascorbate-correlated genes, we arranged the TF-target interaction based on the relative response of correlated genes, i.e., the fold-change difference in expression compared to the fold-change difference in ascorbate concentration (Supplementary Fig. S6), regardless of their type of response (depletion, expected, or excess). Unfortunately, we could not identify any TF subset that could explain a stronger response to ascorbate concentration (Supplementary Dataset S9), suggesting that the observed changes in gene expression cannot be explained solely by the combination of TF targeting these genes, and that additional layers of regulation may be operating in the ascorbate-mediated control of gene expression.

Visualizing Gene Sensitivity to Ascorbate Depletion

Given the intermediate ascorbate deficiency in *vtc4* mutants, we explored gene expression patterns across *vtc4* and *vtc2* to assess gene expression sensitivity to ascorbate depletion. By comparing fold changes in *vtc4* (65% of WT ascorbate) *versus vtc2* (20% of WT), we classified genes based on their depletion sensitivity (Supplementary Fig. S7A and B). Statistical analysis revealed significant enrichment of genes with low or expected sensitivity to ascorbate deficiency (observed 66%, expected 20%), while high-sensitivity genes were underrepresented (observed 33%, expected 79.9%) (Supplementary Fig. S7C and D). Similarly, PCGs and NCGs responding to ascorbate depletion were enriched more than threefold (Supplementary Fig. S7C and D). Considering that *vtc2* mutant does not show obvious developmental defects despite containing 20% of WT content (Lim et al., 2016), and that some Arabidopsis ecotypes have ascorbate concentrations that fall between the levels of Col-0 *vtc2* and Col-0 *vtc4* even under normal growth conditions (Aarabi et al., 2023), the selective conservation of low-sensitivity genes may suggest an evolutionary preference for energy-efficient transcriptional responses unless critical for survival.

Interestingly, as observed in Supplementary Figs. S5A and B and S7A and B, genes with similar ascorbate sensitivity did not necessarily share the same type of response. To integrate these variables, we developed a custom plot (Supplementary Fig. S8A and B),

simultaneously visualizing gene response type (y-axis) and sensitivity to ascorbate depletion (x-axis). Expected responses aligned near the red horizontal line, and expected sensitivities aligned near the blue vertical line. Therefore, genes highly sensitive to depletion positioned towards the right of the vertical blue line (Supplementary Fig. S8C, sectors ii and iv). For example, PCGs like *MYO-INOSITOL OXYGENASE 1* (*MIOX1*) (also in Fig. 3E), *TAA1* (also in Fig. 3G), and *PLANT U-BOX 48* (*PUB48;* also in Supplementary Fig. S9A) exhibited high sensitivity, while most NCGs clustered in sector (i), characterized by an upregulation in *vtc2* but negligible changes elsewhere (Supplementary Fig. S8B and D). Notably, nine PCGs exhibited expected responses and high sensitivity (consisting of *MIOX1* (Fig. 3E), *TAA1* (Fig. 3G), and seven other genes plotted in Supplementary Fig. S9A; see green highlighted genes in Supplementary Dataset S6A). Conversely, only three NCGs met similar criteria (Supplementary Fig. S9B; see green highlighted genes in Supplementary Dataset S6B). These genes had not previously been linked to ascorbate, most likely due to the weak change of expression between the two most contrasting genotypes, *vtc2* and *vtc2/OE-VTC2,* with relative responses ranging between 11-19% (Supplementary Fig. S9). However, genes with stronger relative responses like *DELAY OF GERMINATION 1 (DOG1)* (PCG; Fig. 3E; see blue highlighted genes in Supplementary Dataset S6A), or *AvrRpt2-INDUCED GENE 1 (AIG1), CYSTEINE-RICH RECEPTOR-LIKE PROTEIN KINASE 7 (CRK7)* and *PATHOGENESIS-RELATED GENE 5 (PR5)* (NCG; Fig. 3F; see blue highlighted genes in Supplementary Dataset S6B) are some examples of genes whose change in expression has been recapitulated in other studies of the *vtc2-1* mutant (Gao et al., 2011; Kerchev et al., 2011).

In summary, Supplementary Fig. S8 provides a refined framework for identifying genes with distinct transcriptional responses to ascorbate (Supplementary Dataset S6A and B). Our findings provide a foundation for future research into ascorbate-mediated gene regulation and its implications for redox homeostasis in plant cells.

Expression patterns of PCGs and NCGs reveal a potential link between ascorbate and auxin

Among correlated genes, we identified several PCGs and NCGs involved in different aspects of auxin homeostasis, which is in line with prior studies that suggested that there might be an interaction between ascorbate and auxin in plants (Akram et al., 2017; Bulley et al., 2021; Wang et al., 2021). Among the PCGs of the class “responding to ascorbate as expected” that also showed “high sensitivity to depletion”, we found TAA1, a tryptophan aminotransferase catalyzing the first committed step of auxin biosynthesis (Stepanova et al., 2008; Tao et al., 2008; Yamada et al., 2009), whose expression is reduced in vtc2 and vtc4, and increased in the vtc2/OE-VTC2 line (Fig. 3C and G; Supplementary Figs. S8A and S9A). While other genes involved in auxin biosynthesis were either very poorly expressed or not significantly

correlated with ascorbate concentration, a *TAA1* paralog, *TAR2,* was among genes repressed in *vtc2* but not significantly correlated with ascorbate concentration (Supplementary Fig. S10; Supplementary Dataset S2). In addition, a number of genes involved in auxin signaling and response were also identified among the ascorbate co-regulated genes (Fig. 3G). For example, *IAA17/AXR3,* that encodes an auxin co-receptor (Leyser et al., 1996; Kubalová et al., 2024), and ROOT MERISTEM GROWTH FACTOR 9 (RGF9), encoding a peptide involved in the subcellular regulation of auxin carrier turnover (Whitford et al., 2012), are both PCGs responding to ascorbate depletion (Fig. 3G; Supplementary Figs. S8A and S9A; Supplementary Dataset S6A). Among NCGs, we identified those encoding the ubiquitin-binding protein *TOBAMOVIRUS MULTIPLICATION 1 (TOM1)-LIKE 4* (*TOL4*) involved in subcellular distribution of PIN-type auxin carriers (Korbei et al., 2013) (Fig. 3G) and *AUXIN-INDUCED IN ROOT CULTURES 12* (*AIR12*), an auxin-inducible gene (Neuteboom et al., 1999) that provides cold tolerance by increasing ascorbate concentration, hence counteracting H_2O_2 accumulation (Wang et al., 2021) (Fig. 3G; Supplementary Fig. S8B; Supplementary Dataset S6B). In summary, the changes in expression of genes related to auxin biosynthesis, transport, and signaling point towards a potential crosstalk between ascorbate concentration and auxin patterns of activity.

Exogenous ascorbate induces auxin biosynthesis under continuous light, but not under continuous darkness

Encouraged by prior studies suggesting that ascorbate and auxin may interact (Kerk et al., 2000; Bulley et al., 2021; Wang et al., 2021), and our finding that several genes involved in auxin biosynthesis, signaling, or transport are correlated with ascorbate concentration, we decided to further investigate the relationship between the auxin and ascorbate levels. We focused on *TAA1*/AT1G70560 (also known as *WEAK ETHYLENE INSENSITIVE 8* (*WEI8*)) because it is a key component in auxin biosynthesis implicated in the crosstalk with several hormones and other signals (Stepanova et al., 2008; Tao et al., 2008; Yamada et al., 2009; Zhou et al., 2011; Brumos et al., 2018; Brumos et al., 2020). We chose to perform this work in seedlings (rather than in adult plants which we used for RNA-seq) given that most studies cited above exploring plant defects in auxin biosynthesis or response also looked at seedlings, and we relied on these established phenotypic assays as our reference. We analyzed whether altered ascorbate concentration affects auxin biosynthesis through TAA1 expression by examining the effect of exogenous application of ascorbate on the expression of *TAA1* using the recombineering line *wei8-2/TAA1p:YPet-gTAA1* (backcrossed to WT, previously shown in *wei8-2 tar2-1* background in Brumos et al., 2018). In this line, the *TAA1* promoter (10 kb upstream of the ATG start codon) drives the expression of the yellow fluorescence protein gene *YPet* fused to the N-terminus of the full-length *TAA1* gene

(containing all introns) in its genomic context, inserted in a random location of the *wei8-2* mutant genome (*wei8*/*YPet-gTAA1*). Consistent with the transcriptomic data, the exogenous application of ascorbate to *wei8*/*YPet-gTAA1* seedlings caused the induction of the YPet-TAA1 fusion protein in the epidermis and vasculature in the transition and elongation zones of the root in plants grown under continuous light (Fig. 4A). To determine whether the application of ascorbate also led to increased auxin signaling, we used Arabidopsis lines expressing the synthetic auxin-inducible reporter *DR5:GFP* in WT (Col-0) background (Ulmasov et al., 1997; Weijers et al., 2006). Under control conditions, GFP was detected in the root columella, quiescent center, and vasculature cells. Upon ascorbate supplementation, *DR5:GFP* expression increased in the non-meristematic portion of the root vasculature (Fig. 4B).

We examined whether the *DR5:GFP* expression changes in response to ascorbate in the absence of functional *TAA1*. The *wei8-1* mutant (hereon, *wei8*), whose tryptophan aminotransferase activity encoded by *TAA1* has been knocked-out, showed an overall reduction of *DR5:GFP* signal in control conditions relative to WT, consistent with partially impaired auxin biosynthesis in the mutant (Fig. 4B). However, ascorbate treatment still caused an increase in *DR5* activity in the vasculature in the *wei8 DR5:GFP* line (Fig. 4B) suggesting that ascorbate may regulate the levels and distribution of auxin even in the absence of functional *TAA1*. In contrast to what was seen in seedlings germinated under continuous light, in dark-grown seedlings, the YPet-TAA1 expression and the *DR5:GFP* activity in roots were not affected by exogenous ascorbate (Fig. 4C and D), suggesting that the effect of ascorbate on auxin response in roots may be light-dependent. In light-grown WT seedlings treated with 0.5 mM ascorbate, a ~65% root growth reduction was observed relative to the untreated control, whereas the ascorbate response of hypocotyls was negligible (Fig. 4E and F). Consistent with unaltered levels of *DR5* activity in the dark, and in contrast to light-grown seedlings, dark-grown roots were not prominently affected by the supplementation of growth media with 0.5 mM ascorbate (Fig. 4G and H). Importantly, regardless of light conditions, the reduction of root growth by ascorbate was significantly more prominent in the *wei8* mutant, and the response of roots was reverted to WT values in the complemented line, *wei8*/*YPet-gTAA1* (Fig. 4C, D, G, H). The greater sensitivity to exogenous ascorbate observed in the primary roots of *wei8* mutants was consistently reproduced at lower concentrations of ascorbate in light-grown seedlings (Supplementary Fig. S11). On the other hand, hypocotyl response to ascorbate was unaffected by the genotype in both sets of conditions (Fig. 4C, D, G, H), with enhanced hypocotyl elongation known to be associated with increased auxin activity under standard growth conditions (*superroot2* mutant in Delarue et al., 1998; *YUC1* overexpression in Zhao et al., 2001; *TAA1p:YUC1* transgene in Stepanova et al., 2011; *iaaM* in Romano et al., 1995; and *cyp72ox*

in Zhao et al., 2002). Together, our results show that exogenously applied ascorbate in light-grown seedlings translated into an increase in TAA1 protein accumulation and enhanced auxin response in specific cell types of the primary root.

We considered the possibility that, unintuitively, ascorbate supplementation may as well lead to an intracellular H_2O_2 burst as a consequence of the mechanisms involved in ascorbate transport (Horemans et al., 2000; Mellidou and Kanellis, 2024). Our current understanding of ascorbate transport from the extracellular space is that it is mainly imported as dehydroascorbate (DHA), hence requiring prior oxidation by apoplastic ascorbate oxidase (AO) or ascorbate peroxidase (APX) activities (de Pinto and De Gara, 2004; Mellidou and Kanellis, 2024). Once in the cytosol, DHA is reduced back into ascorbate by DHA reductase (DHAR) at the expense of other relevant molecules involved in the regulation of the cell redox state through the Foyer-Halliwel-Asada cycle such as glutathione (GSH) and NAD(P)H. Therefore, it is theoretically possible that exogenously applied ascorbate may lead to the accumulation of H_2O_2 in root cells due to transient GSH and NAD(P)H decreased concentration. To address this concern, we examined spatial H_2O_2 accumulation in root apical meristem (RAM) and transition zone (TZ) of primary roots under the same experimental setups by quantifying staining intensity of with 3,3'-diaminobenzidine (DAB) (Thordal-Christensen et al., 1997; Daudi and O'Brien, 2012) (Supplementary Figure S12A). Repeated experiments consistently showed smaller or equal DAB staining upon exogenous supplementation with 0.5 mM ascorbate compared to control under any of the light regimes tested, suggesting that no significant amounts of H_2O_2 accumulate at the end of the experiment, in agreement with previously described ascorbate-mediated alleviation of NaCl-induced oxidative stress during germination (Kakan et al., 2021). We considered the possibility that the sensitivity to exogenous ascorbate may be developmental stage-specific and end-point spatial measurements may not record an earlier impact on root growth. To test whether an increase in ascorbate-induced H_2O_2 concentration during an earlier developmental stage underpinned root shortening in light-grown seedlings, we examined the end-point relative root growth of ascorbate-altered lines to exogenous ascorbate (Supplementary Fig. S12B), since ascorbate-defective lines are more sensitive to oxidative stress while usually undistinguishable from WT under control conditions (Huang et al., 2005; Gao and Zhang, 2008; Yu et al., 2019; Hoang et al., 2021; Arnaud et al., 2022). Relative root growth of ascorbate-deficient lines *vtc2* and *vtc4* did not show greater sensitivity to exogenous ascorbate across independent experimental repetitions (Supplementary Fig. S12B).

In summary, we conclude that ascorbate supplementation does not significantly boost H_2O_2 accumulation under our growth conditions and, therefore, ascorbate is likely responsible for

the induction of *TAA1* and the increase of auxin signaling activity, as well as for the root shortening phenotype observed in light-grown seedlings.

TAA1 and *TAR2* have a prominent role in the light-dependent ascorbate-mediated increase in auxin response

To investigate ascorbate-dependent induction of a wider set of auxin biosynthesis genes beyond *TAA1*, we analyzed the expression of its two paralogs, *TAR1* and *TAR2*, and 11 *YUC* genes in response to ascorbate treatment by utilizing Arabidopsis recombineering lines that harbor genomic DNA fusions with *GUS,* and in parallel we employed a *DR5:GUS* reporter to monitor auxin activity (Stepanova et al., 2008; Brumos et al., 2020). Consistent with the results presented above for the *DR5:GFP* reporter (Fig. 4B), in light-grown seedlings, ascorbate supplementation of growth media led to the expansion of the domain of *DR5:GUS* expression in the root vasculature, but not in the hypocotyls (Fig. 5A and B). Likewise, the pattern of *GUS-gTAA1* activity in roots upon ascorbate application in light-grown plants (Fig. 5A) was similar to that observed in the *YPet-gTAA1* line (Fig. 4A), with increased GUS staining in the root elongation zone. Interestingly, in light-grown seedlings, ascorbate treatment also induced the expression of *GUS-gTAR2* (Fig. 5A), a gene encoding the same enzymatic activity as *TAA1* (Stepanova et al., 2008), which could explain the ascorbate-dependent increase of auxin activity in the *wei8* mutant (Fig. 4B). Remarkably, the induction of *TAR2* expression, like that of the *TAA1* and *DR5* reporter lines, was also light-dependent, i.e. not observed in dark-grown seedlings (Fig. 5B). We also found that ascorbate application altered the expression of other auxin biosynthetic genes, such as *YUC5*, *YUC6*, and *YUC8,* in light-grown seedlings (Supplementary Fig. S13A), while only *YUC3* was affected by ascorbate in the dark (Supplementary Fig. S13B). While these results may appear not fully supported by our transcriptomic analysis that failed to detect the effects of endogenous ascorbate levels on *YUC* gene expression (Supplementary Fig. S7), they are not unexpected given the differences in plant age, growth conditions, and tissue types between these experiments and our RNA-seq work. Furthermore, the ascorbate-triggered expression domain changes visualized with the help of auxin reporters are highly spatially restricted and thus are likely to be diluted in samples comprising whole plants analyzed by RNA-seq. Finally, the reporter lines examined in this work harbor translational fusions that could be subject to translational and post-translational regulations not accounted for at the mRNA level.

Considering the prominent ascorbate-induced expression of *TAA1* and *TAR2*, the two major active tryptophan aminotransferase genes, we tested the root growth response to ascorbate of a *wei8-1 tar2-1* mutant (Supplementary Fig. S14). However, this double mutant shows a severe reduction in root growth in control conditions, consistent with a severely compromised tryptophan aminotransferase activity (Supplementary Fig. S14A; Stepanova

et al., 2008) exogenously applied ascorbate severely impacted root growth compared to its individual mutants counterparts (Supplementary Fig. S14A,C). We could not reliably quantify this response given the need to work with a segregating *wei8 tar2/+* population as *wei8 tar2* double homozygotes are fully sterile (Stepanova et al., 2008). To further confirm that *TAA1* and *TAR2* genes are the only genes with prominent tryptophan aminotransferase activity implicated in ascorbate-induced auxin biosynthesis, we characterized the response of the WT, *wei8,* and two different *tar1 tar2* mutants (a stronger *tar1 tar2-1*, and a weaker *tar1 tar2-2*) upon ascorbate supplementation of light-exposed seedlings (Stepanova et al., 2008). While all four genotypes showed similar organ growth in control conditions, *wei8* and both *tar1 tar2* double mutants were hypersensitive to ascorbate in the roots (Fig. 5C and D). Interestingly, the two *tar1 tar2* mutant allele combinations showed an intermediate FC in root length in response to ascorbate that fell between that of WT and *wei8* (Fig. 5C and D). A mild disruption of *TAR2* (*tar1 tar2-2*) led to phenotypes that are slightly more similar to WT, whereas a stronger disruption of *TAR2* (*tar1 tar2-1*) translated into a root length FC more similar to that of *wei8* (Fig. 5C and D).

We then examined in detail the roots of light-grown seedlings to find an interesting observation where exogenously applied ascorbate translated into reduced RAM size in all genotypes, including WT (Supplementary Fig. S14B). Furthermore, ascorbate treatment differentially altered root hair development across mutants, except upon the virtual abolishment of tryptophan aminotransferase activity (*wei8 tar2-1*) when no change was observed (Supplementary Fig. S14B). The developmental changes observed in WT roots upon ascorbate treatment resembled the roots of Arabidopsis lines with ectopic overproduction of auxin under control conditions (Supplementary Fig. S14A,B), supporting that increased ascorbate concentration may lead to increased auxin signaling activity (Fig. 4).

These results, together with our observation that *TAR2*, but not *TAR1*, is expressed in the roots under continuous light and it is induced upon ascorbate exogenous supplementation (Fig. 5A), suggests that both *TAA1* and *TAR2* play a role in the root response to ascorbate. The fact that *wei8* and *tar1 tar2* mutants showed a more severe reduction of root growth after ascorbate treatment than WT implies that auxin is necessary to counteract ascorbate-induced root shortening. Consistently, ascorbate induced the expression of *TAA1* and *TAR2* (Figs. 4A and 5A), leading to an increase of auxin signaling activity.

Tissue-specific auxin gradients are necessary to cope with an increase in ascorbate concentration

In light of these results, we tested whether exogenous supplementation with IAA could improve root growth of WT and auxin-deficient seedlings in the presence of ascorbate. To do that, we analyzed the relative root length of WT, *wei8,* and *aux1-7* (hereon, *aux1*, an auxin-insensitive mutant defective in IAA uptake into the cells; Bennett et al., 1996) in light-grown seedlings germinated in the presence of 0.5 mM ascorbate either with or without supplementation with 100 nM IAA (Fig. 6A and B). We observed that the root lengths of WT, *wei8* and *aux1* plants in control conditions (no ascorbate) remained unchanged in the presence of 100 nM IAA (Fig. 6A). However, we found that 100 nM IAA partially alleviated the inhibitory effect of 0.5mM ascorbate on WT root growth (Fig. 6B). This effect was also observed in the mild auxin-deficient mutant *wei8* but not in an auxin mutant defective in auxin import, *aux1*. Interestingly, the relative root length in IAA plus ascorbate in *wei8* was shorter than that of WT, suggesting that the low auxin levels of *wei8* may not be the only reason for the short root phenotype of this mutant in the presence of ascorbate. We reason that exogenously applied IAA may not result in the same IAA distribution patterns or gradients as those produced by the combination of *TAA1*-mediated local auxin production in response to ascorbate and auxin transport.

It is known that IAA enters the cells mainly by auxin influx carriers like AUX1 and LIKE AUXIN RESISTANT (LAX) (Swarup and Bhosale, 2019). To investigate the potential role of auxin influx in the root response to ascorbate, we analyzed the relative root growth inhibition caused by 0.5 mM ascorbate in WT, *wei8,* and the auxin import-deficient mutant *aux1* (Fig. 6C). Relative growth of *aux1* roots in the presence of ascorbate was comparable to that of *wei8* despite the presence of a fully functional auxin biosynthesis pathway in *aux1* (Fig. 6A to C), suggesting that auxin cell-to-cell transport is necessary besides IAA biosynthesis. However, our RNAseq results performed in adult rosettes did not show differences in gene expression for *AUX1* and other auxin importers such as *LAX1-LAX3*, as well as of auxin exporters like *PIN-FORMED* (*PIN*) genes (Supplementary Fig. S15). Furthermore, as expected for an auxin influx mutant, the root growth inhibition caused by ascorbate in *aux1* could not be rescued by exogenous IAA supplementation (Fig. 6B). These results highlight the importance of auxin biosynthesis and transport as a coping mechanism against the physiological impact of increased ascorbate concentration.

Discussion

In this study, we used previously characterized strong (*vtc2*) and weak (*vtc4*) ascorbate-deficient mutants, WT, and a generated high-ascorbate transgenic line in which the uORF-less *VTC2* CDS is constitutively expressed, to examine the effect of altered concentrations

of ascorbate on the Arabidopsis transcriptome. Ascorbate status had little effect on transcripts associated with the ascorbate biosynthesis *via* the mannose-L-galactose pathway or on ascorbate recycling enzymes. Similarly, increasing ascorbate by feeding ascorbate or its precursor L-galactono-1,4-lactone did not influence expression of ascorbate-related genes (Bulley et al., 2009; Gao et al., 2011).

The range of endogenous ascorbate concentrations in the lines studied in this work, in combination with their genome-wide transcriptomic profiles, led us to identify: (i) genes whose expression is significantly different under distinct ascorbate concentrations when compared to WT (DEGs), and (ii) genes whose expression correlates with ascorbate concentration across genotypes (PCGs and NCGs). Both *vtc2* and *vtc4* mutants showed strong reductions in the expression of *VTC2* (47-fold) and *VTC4* (75-fold) respectively and, noteworthy, we found reduced *VTC2* mRNA levels in the *vtc2/OE-VTC2* line. We hypothesize that it might be the consequence of partial transgene silencing, either due to its co-suppression in the presence of the *vtc2* mutant T-DNA (SAIL_769_H05) (Daxinger et al., 2008; Mlotshwa et al., 2010), or due to a transcriptional or post-transcriptional downregulation of the transgene (e.g., via reduced transcription or enhanced mRNA degradation) by the plant in an attempt to maintain ascorbate homeostasis.

The *vtc2* transcriptome was the most divergent from WT among all lines analyzed (Fig. 2A, C; Supplementary Fig. S3A; Supplementary Dataset SS4), with most DEGs unique to *vtc2*, whereas *vtc4* and *vtc2/OE-VTC2* shared over 60% of their DEGs (Fig. 2B, E; Supplementary Dataset SS4). Comparison with a previous dataset based on the EMS allele *vtc2-1* grown under similar conditions to those in our study (Kerchev et al., 2011) revealed only 37% overlap (Supplementary Fig. S16), likely due to differences in alleles, profiling platforms, and statistical thresholds, as well as the presence of a cryptic mutation in *vtc2-1* (Lim et al., 2016). To identify consistent transcriptional changes, we defined a core set of *vtc2* DEGs reproducibly altered in both datasets (Supplementary Dataset S10).

Gene ontology analysis indicated that *vtc2* displays suppressed abiotic stress responses and enhanced defense-related transcriptional programs, consistent with previous reports linking ascorbate deficiency to elevated ROS, salicylic acid accumulation, and increased resistance to biotrophic pathogens (Barth et al., 2004; Pavet et al., 2005; Mukherjee et al., 2010). Supporting this notion, numerous *WRKY* transcription factors were induced in *vtc2*, while *vtc4* exhibited a much weaker response (Supplementary Dataset S2-4). Some of these regulatory hubs, like *WRKY46*, involved in basal resistance to *Pseudomonas syringae* (Hu et al., 2012), or like *WRKY18*, *WRKY33*, or *WRKY40*, which integrate ROS and hormone signaling

activity to maintain redox homeostasis (Liu et al., 2015; Birkenbihl et al., 2017; Birkenbihl et al., 2017; Andrade Galan et al., 2025) showed significant TFBS enrichment among ascorbate-correlated genes promoters (Supplementary Dataset S6C, D), suggesting that altered ascorbate status modulates WRKY-dependent defense networks. However, integration of DAP-seq binding data (O'Malley et al., 2016) with our expression profiles showed that WRKY-targeted genes did not respond proportionally to ascorbate levels (Supplementary Fig. S5D; Supplementary Materials 7 and 8), indicating that WRKYs are unlikely to directly mediate ascorbate-dependent transcriptional adjustments. Given the close interaction between WRKYs and ROS signaling stated above, these changes may instead reflect redox-driven transcriptional reprogramming rather than direct effects of ascorbate. While our data does not identify specific transcriptional regulators linking ascorbate status to gene expression, they highlight WRKY factors as central components of the response to altered ascorbate homeostasis, meriting further investigation.

The transcript levels of genes directly involved in ascorbate biosynthesis, catabolism, recycling, or regulation were largely unaffected by ascorbate. However, we identified 197 genes whose expression was significantly altered in the *vtc2* mutant but was rescued to WT level upon *VTC2* overexpression (Fig. 3A–D; Supplementary Dataset S6A and B): 90 PCGs and 107 NCGs. Among the PCGs with the strongest response, we identified both uncharacterized genes, such as *AT5G11330* (*FAD/NAD(P)-BINDING OXIDOREDUCTASE*), and genes with known functions. Notably, *DOG1* (Fig. 3E; Supplementary Dataset S6A) showed a positive correlation with both endogenous ascorbate levels and exogenously applied L-galactono-1,4-lactone. While *DOG1* is a well-characterized regulator of seed dormancy (Graeber et al., 2014; Footitt et al., 2020; Krüger et al., 2025), this study presents a functional link between it and ascorbate. We also observed a strong positive response in *MIOX1*, which encodes an enzyme proposed to increase ascorbate biosynthesis (Lorence et al., 2004). However, its relevance in ascorbate biosynthesis remains debated due to conflicting reports (Endres and Tenhaken, 2009). The strongest relative responses among NCGs (Fig. 3F; Supplementary Dataset S6B) were led by two biotic stress-related genes—*AIG1* (Reuber and Ausubel, 1996; Wang et al., 2019) and *PR5* (Uknes et al., 1992; Thomma et al., 1998; Seo et al., 2008)—along with the uncharacterized genes *AT3G15536* and *AT5G13320*. The genes listed in Supplementary Dataset S6 represent a valuable group of candidates to prospect for putative regulatory elements. Understanding the molecular mechanisms underpinning these correlations could open the door to building synthetic ascorbate-responsive reporters.

The increasing interest in ascorbate regulation (Conklin et al., 2013; Laing et al., 2015; Fenech et al., 2021; Aarabi et al., 2023; Bournonville et al., 2023) suggests a potential interplay with hormone signaling. Our gene expression profiling analysis, which identified genes correlating with ascorbate concentration, revealed a significant enrichment of auxin-related genes among the PCGs. These include the key auxin biosynthetic gene *TAA1* (Stepanova et al., 2008; Tao et al., 2008; Yamada et al., 2009), along with *RGF9* (Whitford et al., 2012), *IAA17* (Leyser et al., 1996; Kubalová et al., 2024), *TOL4* (Korbei et al., 2013), and AIR12 (Neuteboom et al., 1999; Wang et al., 2021) (Fig. 3G; Supplementary Figs. S8 and S9). To validate the connection between ascorbate and auxin, we examined the effect of exogenous ascorbate on the expression of TAA1, a rate-limiting enzyme in tryptophan-dependent auxin biosynthesis. Using the complemented Arabidopsis *wei8* mutant expressing a *TAA1p:YPet-gTAA1* construct, we observed a light-dependent, concomitant increase in YPet-TAA1 signal and *DR5* activity in response to increased ascorbate concentration (Fig. 4A and D). This validated our transcriptomic finding that *TAA1* expression is positively correlated with endogenous ascorbate levels (Fig. 3C; Supplementary Figs. S8A and S9A). This result is also consistent with a previous report showing that L-galactose or ascorbate supplementation slightly increased auxin levels in Arabidopsis (Bulley et al., 2021).

We further investigated the role of other auxin biosynthetic genes. Interestingly, even in the absence of TAA1 activity, ascorbate treatment still triggered an increase in auxin response (Fig. 4B). We found that the *TAA1* paralog, *TAR2* (but not *TAR1*), also displayed a light-dependent increase in expression upon exogenous ascorbate supplementation (Fig. 5A and B). Furthermore, the effect of ascorbate on root growth in *tar1 tar2* double-mutant alleles was intermediate between WT and *wei8* (Fig. 5C and D), confirming that *TAR2* is likely responsible for the residual ascorbate-mediated *DR5* induction in the *wei8* mutant. While the ascorbate-mediated effect on *TAA1* expression was light-dependent, we observed a mild reduction of root growth in the *wei8* mutant in response to ascorbate in both light- and dark-grown plants (Fig. 4F and H). This suggests that both light and basal auxin levels are important for modulating ascorbate's effects on root length. Consistent with the idea that auxin is required to cope with excessive ascorbate, exogenous IAA supplementation alleviated the root growth defects in both WT and wei8 mutants on ascorbate-supplemented plates. This rescue was dependent on a functional auxin influx carrier, as the aux1 mutant was not complemented by exogenous IAA (Fig. 6B). However, neither exogenous IAA (Fig. 6) nor ectopic auxin overproduction (Supplementary Fig. S14) restored the ascorbate-induced root growth inhibition in *wei8* roots. This led us to hypothesize that auxin distribution, rather than overall concentration, is critical for the plant's response to elevated ascorbate levels.

The observation that ascorbate-mediated root growth inhibition is similar in *wei8* and the auxin transport mutant *aux1* (and stronger than in WT) suggests that both local auxin production and transport are essential for a normal response to ascorbate. Specifically, the root requires a functional AUX1 carrier to deliver IAA from the auxin-source cells (where *TAA1/TAR2* activities are induced by high ascorbate) into the auxin-sink cells. This model aligns with reports indicating that a combination of local biosynthesis and transport is necessary to establish morphogenic auxin gradients (Brumos et al., 2018), which, in our case, ensures a proper response to increased ascorbate. Therefore, alterations in local auxin production (*wei8*) or auxin influx (*aux1*) result in an enhanced ascorbate root inhibition response (Fig. 6). The identification of *TAA1* and *TAR2* as ascorbate-regulated auxin biosynthesis genes, along with the requirement for the AUX1 influx carrier, pinpoints a boost in local auxin production and the maintenance of its distribution as exciting players in the root response to ascorbate excess in light-grown seedlings. Further work is required to pinpoint the exact cells requiring auxin to cope with excessive ascorbate.

Several questions arise from the results presented in this study related to what molecular mechanism underpins ascorbate-mediated boost of auxin biosynthesis and distribution, and, importantly, whether there is one or multiple signaling mechanism involved. We first discarded the possibility that the signaling trigger was H_2O_2 accumulation resulting from ascorbate intake, based on DAB staining and root phenotyping of ascorbate-deficient lines (Supplementary Fig. S12). Considering ascorbate concentration as the actual trigger, it was reasonable that ascorbate concentration was directly involved in the phenotypes described in this study. At the same time, we also report here that two genotypes with mild contrasting concentrations of ascorbate—*vtc4* and *vtc2/OE-VTC2*—showed overlapping transcriptomes (Fig. 2E; Supplementary Fig. S4), suggesting that mechanisms more complex than a direct [ROS]- or [ascorbate]-mediated signaling pathway may be involved. Ascorbate can be transported in and out the cell (Horemans et al., 1998; Horemans et al., 2008; Liao et al., 2025), and therefore, the redox state of both the cytosol and the apoplast are potentially susceptible to changes in ascorbate concentration. Building on proposed ascorbate-regulated signaling models (Pignocchi and Foyer, 2003; Mellidou and Kanellis, 2024), we propose that increased apoplastic ascorbate translates into a reduced apoplastic ROS concentration via the activities of Ascorbate Oxidase (AO) and Ascorbate Peroxidase (APX) (Pignocchi and Foyer, 2003; de Pinto and De Gara, 2004) (Fig. 7A). This decrease in the H_2O_2 signal is transmitted to the nucleus (e.g., *via* HPCA1 (Wu et al., 2020; Fichman et al., 2022) or AHK5 (Drechsler et al., 2025) systems), leading to transcriptional changes in PCGs and NCGs, potentially regulated by WRKY transcription factors (Liu et al., 2015; Birkenbihl et al., 2017; Andrade Galan et al., 2025) (Fig. 7A). The known link between auxin and ROS—where

auxin signal transduction promotes ROS production in the cell wall to drive cell elongation (Schopfer et al., 2002; Krishnamurthy and Rathinasabapathi, 2013; Peer et al., 2013), and, reciprocally, ROS regulates auxin distribution (Pasternak et al., 2023)—provides a plausible framework. Our observations that *RGF9* and *TOL4* (involved in auxin spatial distribution) correlate with ascorbate concentration (Fig. 3G and Supplementary Fig. S9A), and that root shortening upon ascorbate treatment is associated with smaller root cell size (due to potential cell wall stiffening; Supplementary Fig. S14B), are consistent with this model. We hypothesize that increased ascorbate concentration leads to decreased ROS accumulation, which impairs cell elongation. This signal is perceived in the nucleus, promoting increased *de novo* auxin biosynthesis that promotes local and distant accumulation of apoplastic ROS (Fig. 7B), hence compensating for the initial altered ROS concentration that may have disrupted normal auxin distribution (Pasternak et al., 2023).

We have gathered enough evidence to partially explain the ascorbate mechanism of action via the tuning of ROS concentration. However, a major paradox remains: how these ROS-mediated mechanisms are interwoven to yield ascorbate-correlated genes while simultaneously producing convergent transcriptomes in genotypes with contrasting ascorbate levels (*e.g.*, *vtc4* and *vtc2/OE-VTC2*)? This suggests the involvement of complex, dose-independent regulatory mechanisms. To resolve this paradox, we initially considered three hypotheses: (1) Ascorbate overproduction in *vtc2/OE-VTC2* and the mild deficit in *vtc4* may lead to compensatory transport patterns that ultimately result in similar ascorbate accumulation in specific subcellular spaces (apoplast, cytosol, or vacuole). If signaling is localized, this shared concentration would explain the transcriptome overlap; (2) Both genotypes might converge in the accumulation of the ascorbate precursor GDP-L-galactose (Figure 1A) due to either an enzymatic bottleneck (*vtc4*) or a high metabolic flux (*vtc2/OE-VTC2*). However, evidence from metabolic simulations and *VTC2/VTC4* overexpression in *Nicotiana benthamiana* suggests that *VTC4* activity is not limiting upon *VTC2* overexpression, making it likely that GDP-L-galactose is efficiently channeled toward ascorbate biosynthesis in the *vtc2/OE-VTC2* line (Fenech et al., 2021). This makes precursor accumulation an unlikely primary driver of the convergence. (3) The observation that ~80% of PCG and NCG show significant enrichment in epigenetic marks (Supplementary Dataset S6C, D) makes it tempting to speculate that part of ascorbate's mechanism of action may be mediated by tuning the activity of epigenetic machinery—a mechanism described in animal cells (Blaschke et al., 2013; Minor et al., 2013). This could impose a shared layer of regulation that overrides the overall concentration differences.

We believe that this uncovered link between ascorbate and auxin, along with the identification of ascorbate-correlated genes, will catalyze future research into how these two environment-responsive signaling pathways are integrated to regulate plant development, and shed light on broader roles of ascorbate in other biological processes.

Materials and methods

Plant Materials

All Arabidopsis (*Arabidopsis thaliana*) lines used in this study are of Col-0 ecotype (WT). Arabidopsis lines employed in this work that have been described previously include: *vtc2/GPPp:GPP-GFP L13 ,* herein referred to as *VTC2p:VTC2*$_{CDS}$*-GFP* (Fenech et al., 2021); *vtc2-4,* herein referred to as *vtc2* (SAIL_769_H05; Lim et al., 2016); *vtc4-4*, herein referred to as *vtc4* (SALK_077222; Torabinejad et al., 2009); *wei8-1, wei8-2, tar1-1, tar2-1* and *tar2-2* mutants and their higher order combinations (Stepanova et al., 2008) and *aux1-7* mutant was previously described and characterized (Bennett et al., 1996; Marchant et al., 1999; Marchant et al., 2002). The generation of transgenic lines *vtc2/OE-VTC2* L15 and L16 for this work is described below. Recombineering line *wei8-2/TAA1p:YPet-gTAA1* was generated after backcrossing it to WT and segregating *tar2-1* out from the original line (ABRC stock #CS72246; Brumos et al., 2018; Brumos et al., 2020b) in this work. Auxin-inducible synthetic reporter *DR5:GFP* in WT and *wei8* backgrounds (Brumos et al., 2018), *GUS* recombineering lines for *TAR* and *YUC* auxin biosynthesis genes (Brumos et al., 2020), and auxin overproducing lines (YUCox (Zhao et al., 2001); *sur2* (Delarue et al., 1998; Stepanova et al., 2005); *wei8-1 sur2* (Stepanova et al., 2008; Fenech et al., 2025)) were also previously published.

Plasmid construction and generation of transgenic plants

The coding sequence (CDS) of *VTC2* (without stop codon) was PCR amplified from Col-0 cDNA using Phusion High-Fidelity DNA Polymerase (New England Biolabs) and the attB1-VTC2-F (5'-GGGGACAAGTTTGTACAAAAAAGCAGGCTATGTTGAAAATCAAAAGAGTTCC-3') and attB2-VTC2-R (5'-GGGGACCACTTTGTACAAGAAAGCTGGGTGTTCTGAAGGACAAGGCACT-3') primers. The resulting PCR product was recombined by the BP reaction into the pDNOR221 vector (Invitrogen) following manufacturer's instructions. The *VTC2* CDS was then subcloned by LR reaction in the gateway pGWB5 vector (Nakagawa et al., 2007) to produce the *35S:VTC2-GFP* construct. The fidelity of the construct was confirmed by sequencing. Arabidopsis *vtc2* mutant (SAIL_769_H05; Lim et al., 2016) was transformed using the GV3101 strain of *Agrobacterium tumefaciens* using the floral dip protocol (Clough and Bent, 1998). Transgenic lines were screened for 3:1 segregation on half-strength Murashige-Skoog

(M5524 Sigma-Aldrich) plates containing 20 µg/mL Hygromycin (Invitrogen) and propagated to homozygous T3 lines. 16 independent lines were screened and two lines showing high ascorbate content were selected.

Growth conditions

For RNA-seq analysis, Arabidopsis seeds were surface sterilized using chlorine gas by pouring 3 mL of 37% HCl into 100 mL of commercial bleach in a flask and incubated in an airtight sealed container for 4 hours. Then, seeds were aired for at least 4 hours in a laminar flow cabinet and stored at 4ºC for a three-day stratification. Seeds were sown on horizontal half-strength MS (M524 PhytoTech Labs, USA) agar (0.6% [w/v]) (A0949 PanReac Applichem ITW Reagents), pH 5.7 plates supplemented with 1.5% [w/v] sucrose under sterile conditions and grown with a long-day photoperiod (16-h light/8-h darkness cycle, 22±1ºC, 150±50 µmol photons m^{-2} s^{-1}) for 7 days. Seedlings were then transferred to soil (4:1 (v/v) soil:vermiculite) in a semi-randomized order. Rosettes of four-week-old plants grown under short-day photoperiod (8-h light/16-h darkness cycle, 22±1ºC, 300±70 µmol photons m^{-2} s^{-1}) were collected 30 minutes after the lights were turned on and flash-frozen in liquid nitrogen. RNA from three independent replicates per genotype was extracted following the protocol described below.

For ascorbate- and auxin-related experiments, Arabidopsis seeds were surface-sterilized using a sterilization solution (50% commercial bleach (Pure Bright germicidal ultra bleach), 0.02% (v/v) Triton X-100 (Pharmacia Biotech code no. 17-1315-01)) for 5 minutes and washed four times with sterile deionized water. Seeds were stratified for three days at 4 ºC, sown after resuspending them in low-melting point agarose (0.7%) in water on horizontal full-strength Murashige-Skoog (MS) (Caisson Labs ref. MSP01-100LT) agar (0.6% [w/v]) (Difco agar granulated ref. 214510), pH6 supplemented with 1% [w/v] sucrose, and kept for two hours at room temperature to induce germination. The pH of ascorbate-supplemented medium was adjusted to 6 using extra empirically determined 1 M KOH to accommodate 0.5 mM ascorbate, and equivalent volume of 1 M KCl was added to control medium. This medium was autoclaved and cooled down at room temperature before adding filter-sterilized ascorbic acid (Sigma-Aldrich ref. A5960) using 0.22µM filters for aqueous solutions (Millex-GV, Polyvinylidene fluoride (PVDF) ref. SLGV013SL) or indole-3-acetic acid (Sigma ref. I-2886) using dimethylsulfoxide (DMSO)-compatible filters (Choice Polypropylene Syringe Filters ref. CH2225). Plates with seeds for the dark experiment were then transferred to a dark chamber at 22 ºC and incubated for 72 hours. Plates with seeds for the light experiment were transferred to a light walk-in chamber and incubated under continuous LED light (70-100 µmol photons m^{-2} s^{-1}; 2x 6000K Kihung T8 LED integrated fixture 40 W + 1x FULL SPECTRUM Monios-L LED grow light full spectrum 60 W) for 5 days.

Experimental procedures

Ascorbate concentration was determined using an ascorbate oxidase activity assay as previously described (Fenech et al., 2021). Briefly, fresh tissue was homogenized using liquid nitrogen-cold mortar and pestle and extracted with cold 3% (w/v) metaphosphoric acid + 1 mM EDTA, then centrifuged to isolate the supernatant. Absorbance at 265 nm was measured in a UV-transparent plate (Greiner UV-Star 96-Well Microplate) after mixing the samples with either phosphate buffer (0.2 M KH_2PO_4, pH 7), followed by the addition of ascorbate oxidase (AO) and incubation. Changes in absorbance before and after the addition of AO were compared to a standard curve (0–1 mM) to quantify ascorbate content. Confocal imaging was performed using Carl Zeiss LSM710 (excitation: argon laser 488 nm; detection: 499 nm-562 nm) and brightness/contrast was adjusted using FIJI (Schindelin et al., 2012). For GUS histochemical staining of auxin biosynthesis recombineering lines and *DR5*, seedlings were fixed in 90% (v/v) acetone and stained for 48 hours as previously described (Stepanova et al., 2005). Seedling images were acquired using a Q-IMAGING MicroPublisher 5.0 RTV camera coupled to a LEICA MZ125 stereo microscope, and GUS-stained seedlings were imaged using a Diagnostic Instruments Spot Insight 4 14.2 color mosaic Camera coupled to a Carl Zeiss Axioplan microscope. Seedling images and organ size measurements were acquired using an Epson Perfection V600 Photo scanner and analyzed with FIJI/ImageJ.

RNA extraction

RNA from three independent replicates per genotype, where each biological replicate was composed of 8 randomized rosettes, was extracted with Trizol following the manufacturer's protocol. RNA quality and integrity were validated using the Bioanalyzer 2100 (Agilent Technologies Santa Clara, CA, USA), with the RNA integrity number (RIN) of >8.0 for all biological replicates.

RNA-seq differential expression and bioinformatics analysis

Paired-end Illumina mRNA libraries were generated using the TruSeq stranded mRNA kit according to the manufacturer's instructions (Illumina Inc., San Diego, CA, USA) for the mutant and control lines. Libraries were sequenced in an Illumina NextSeq550 platform, and 2 x 75 bp paired-end reads were generated.

The reads were quality-filtered and trimmed using Trimmomatic version 0.36 (Bolger et al., 2014) with paired-end mode options: -threads 8 -phred33 ILLUMINACLIP:TruSeq3-PE.fa:2:30:10:2:True LEADING:3 TRAILING:3 MINLEN:36. The resulting reads were then aligned to the TAIR10 version of the *Arabidopsis thaliana* genome sequence (https://www.arabidopsis.org/) using Hisat2 version 2.1.0 (Kim et al., 2015). These read

alignments (in BAM format) were used for transcript quantification with the Cuffdiff program of the Cufflinks version 2.2.1 package (Trapnell et al., 2013). The resulting read alignments were visualized and clustered using Tablet software (Milne et al., 2013) and CummeRbund R package version 2.23.0 (Goff et al., 2014). To determine DEGs, a q-value<0.05 cutoff was set. For DEGs analysis, genes identified as ID ENSRNA were filtered out.

Principal Component Analysis (PCA) and volcano plot of RNA-seq datasets

To explore the relationship between fold-change and significance (q-value<0.05), Volcano plots were generated using the CummeRbund R package version 2.23.0 (Trapnell et al., 2012). PCA was made using a customized pipeline in RStudio using ggplot2 (Wickham et al., 2025a) and ggfortify (Horikoshi et al., 2024) R packages.

Gene ontology (GO) categories analysis

The PANTHER database (http://go.pantherdb.org/tools/compareToRefList.jsp) was used to obtain the GO biological processes overrepresented in the input gene list (DEGs of a given mutant), using as reference list all *Arabidopsis thaliana* genes annotated in the PANTHER database (Mi et al., 2019; Thomas et al., 2022). The Fisher's exact test with the FDR correction as calculated by the Benjamini-Hochberg procedure was used and only results with FDR<0.05 were selected for further analysis.

Venn diagram analysis and statistical analysis of the overlap

The Venn diagram analysis was performed using "InteractiVenn" and on-line interactive Venn diagram tool and introducing the list of induced and repressed genes for each mutant as input (http://www.interactivenn.net/index.html#) (Heberle et al., 2015).

The statistical significance of the overlap between two groups of genes was calculated using an online tool (http://nemates.org/MA/progs/overlap_stats.html). The complete description of how the enrichment (representation factor) and the associated probability (p-value) were calculated can be found in this web page (http://nemates.org/MA/progs/representation.stats.html).

Correlation analysis

We filtered out genes with Fragments Per Kilobase of transcript per Million mapped reads (FPKM)<1 in at least one of their replicates, and we kept the genes whose average FPKM values followed the desired pattern of *vtc2*>*vtc4*>WT>*vtc2/OE-VTC2* to find NCGs, or *vtc2*<*vtc4*<WT< *vtc2/OE-VTC2* to find PCGs. To do that, we wrote a pipeline in RStudio

utilizing dplyr (Wickham et al., 2023), R.utils (Bengtsson, 2025), and stats R packages (R Core Team, 2025). We performed Pearson's correlation analysis with no transformation to extract genes whose response to ascorbate is linear (FPKM=±m*[ascorbate]+n). Additionally, we performed the same analysis after transforming FPKM values into Napierian logarithm (ln(FPKM)= =±m*[ascorbate]+n) for exponential response, and in the case of NCGs, we also transformed ascorbate concentration into 1/[ascorbate] to identify genes whose expression is inversely proportional to ascorbate concentration (FPKM value positively correlates with 1/[ascorbate]). Best fit for each gene is shown in Supplementary Dataset S5.

Hierarchically clustered TF-target heatmap

This analysis was made using a customized pipeline in RStudio. First, we downloaded the TF-target interactions dataset published by O'Malley et al., 2016. Then, we processed transcription factor (TF) binding data, utilizing the dplyr package (Wickham et al., 2023) for data manipulation, in naïve/methylated (labelled as "col") and unmethylated (labelled as "colamp") DNA to create a TF-target gene database. Finally, we constructed a binary interaction matrix of TF-target pairs for hierarchical clustering using the methylated database. To do this, a matrix was initialized where rows represent target genes and columns represent TFs, with each cell indicating whether a TF binds to a target gene. The matrix was populated with 1 if a TF binds to a target gene and 0 if no binding is detected. To visualize these interactions, the binary matrix was converted into a heatmap using the ComplexHeatmap package in R (Gu et al., 2016; Gu, 2022), with a color gradient distinguishing binding (dark color) from non-binding (light color). Hierarchical clustering was applied to group TFs, while target genes were arranged based on their *vtc2* expression fold-change.

Development of a custom plot to visualize changes in gene expression in response to ascorbate concentration

We hypothesized that, if the expression of an ideal gene (measured as FPKM) was directly proportional to the concentration of ascorbate responding as 1:1, its expression across genotypes would follow two different models: a linear model for a PCG ($\mathrm{FPKM}_{genotype} = \mathrm{m} * [\mathrm{ascorbate}]_{genotype}$, with $\mathrm{m} = \frac{\mathrm{FPKM}_{\mathrm{WT}}}{[\mathrm{ascorbate}]_{\mathrm{WT}}}$), and an inverse model for a NCG ($\mathrm{FPKM}_{genotype} = \mathrm{m} * \frac{1}{[\mathrm{ascorbate}]_{genotype}}$, with $\mathrm{m} = [\mathrm{ascorbate}]_{\mathrm{WT}} * \mathrm{FPKM}_{\mathrm{WT}}$). Using this, we predicted that in the *vtc2* mutant (20% of WT ascorbate), this PCG's expression would be 0.2 times that of WT, while in *vtc2/OE-VTC2* (165% of WT ascorbate), it would be 1.65 times higher. Conversely, an ideal NCG would show 5-fold higher expression in *vtc2* and 0.61-fold in *vtc2/OE-VTC2* (inverse values). In log2 scale, genes with fold changes of (-2.32, 0.72) for

PCGs or (2.32, -0.72) for NCGs would be considered correlated 1:1. The red line in Supplementary Fig. S5A and B represents all theoretically possible genes responding to ascorbate concentration more weakly than a 1:1, but still keeping a balanced proportion between *vtc2* and *vtc2/OE-VTC2* , and genes falling on this line are considered to respond to ascorbate as expected. To experimentally identify these genes, we established a confidence interval based on the highest and lowest observed ascorbate fold changes in *vtc2* and *vtc2/OE-VTC2*, assuming that the true mean could be any of the three measured values per genotype. This confidence range, determined by comparing extreme ascorbate values across replicates, defined two boundary points, and the lines connecting (0,0) to these points represent the upper and lower empirical response limits. The same rationale was utilized to build the plots displayed in Supplementary Fig. S7A and B. Then, both plots were combined in Supplementary Fig. S8A and B, by representing the slope values that each gene had in Supplementary Fig. S5A and B (represented in y-axis) and Supplementary Fig. S7A and B (represented in x-axis). All visual representations of gene expression in response to ascorbate concentration were performed in RStudio utilizing dplyr (Wickham et al., 2023), ggplot2 (Wickham et al., 2025a), ggpubr (Kassambara, 2023a), svglite (Wickham et al., 2025b), and viridisLite (Garnier et al., 2024) R packages.

DAB staining procedure

The presence of H_2O_2 in Arabidopsis roots was detected using DAB (3,3'-diaminobenzidine; Sigma-Aldrich, USA) as previously described (Thordal-Christensen et al., 1997) with modifications. A DAB-HCl solution (pH 3.8, final concentration of 1 mg/mL DAB, Sigma #D-8001) was freshly prepared two hours before use to ensure complete dissolution of the DAB. The seedlings were vacuum-infiltrated in the DAB solution for two cycles of three minutes and subsequently incubated at room temperature in the dark for 15 minutes. Then, the samples were washed three times in a bleaching solution (ethanol:lactic acid:glycerol, 3:1:1, v/v/v) at room temperature for 10 minutes. After that, the samples were transferred to a 60% glycerol solution. The stained plants were imaged using a Zeiss Axio Scope A1 vertical microscope equipped with an AxioCam503 Color camera and Zeiss Zen Blue software.

DAB staining intensity was quantified adapting a previously described method (Carril et al., 2020) as follows. Captured images were imported into FIJI software (Schindelin et al., 2012) and loaded as a hyperstack. The loaded images were first converted to 8-bit and then to RGB color. The images were then submitted to the "Color Deconvolution" plug-in using the built-in FIJI H DAB vector to separate the brown DAB signal from the other colors in the image. The pixel values of the deconvoluted image showing the DAB brown precipitate in a separate channel were inverted to obtain an 8-bit image in which zero represents total white (no brown signal) and 255 represents deep brown (the highest brown signal). The region of interest (ROI)

was established by a rectangle manually adjusted to RAM and TZ. While RAM ROI was adjusted for each image from the root tip until the first elongating cell, the same TZ ROI was used for all images. Then, the mean intensity of brown staining (DAB precipitate) within the ROI was calculated.

Statistical analysis

We made different *ad hoc* pipeline scripts in R to perform statistical analyses utilizing car (Fox and Weisberg, 2019), pwr (Champely et al., 2020), rstatix (Kassambara, 2023b), dunn.test (Dinno, 2024), and multcompView (Graves and Dorai-Raj, 2024) packages. Firstly, we tested whether the dataset was normally distributed (Shapiro-Wilk test) and homoscedastic (Levene test) prior to running the hypothesis contrast analyses. If a dataset was homoscedastic but had strong statistical power (power=1 – β > 0.8, with β being the probability of accepting the null hypothesis when it is actually false), we performed ANOVA followed by post-hoc Tukey test for α=0.05. If not meeting the previously stated requirements, we transformed the data using $\log_{10}$ and retested for homoscedasticity and power. If after data transformation the requirements were not met, we performed non-parametric Kruskal-Wallis test, followed by Dunn's test for α=0.05. For Two-Way ANOVA on RANKS, we performed Aligned Rank Transform for Nonparametric Factorial ANOVA (Kay et al., 2025).

Accession Numbers

Sequence data from this article can be found in the GenBank/EMBL data libraries under accession numbers *AT4G26850 (VTC2), AT3G02870 (VTC4), AT1G70560 (TAA1), AT1G23320 (TAR1), AT4G24670 (TAR2), AT4G32540 (YUC1), AT4G13260 (YUC2), AT1G04610 (YUC3), AT5G11320 (YUC4), AT5G43890 (YUC5), AT5G25620 (YUC6), AT2G33230 (YUC7), AT4G28720 (YUC8), AT1G04180 (YUC9), AT1G48910 (YUC10), AT1G21430 (YUC11)*. Differentially expressed genes' accession numbers are available in Supplementary Dataset S2. PCGs' and NCGs' accession numbers are available in Supplementary Dataset S6. _.

Data availability

The data generated in this publication have been deposited in NCBI's Gene Expression Omnibus (Edgar et al., 2002) and are accessible through GEO Series accession number GSE296827 (https://www.ncbi.nlm.nih.gov/geo/query/acc.cgi?acc=GSE296827). All R scripts utilized to analyze and plot correlation and postcorrelation analyses are available in GitHub (published version doi: 10.5281/zenodo.15587122; concept doi (all versions): 10.5281/zenodo.15424809) through www.doi.org (for example, www.doi.org/10.5281/zenodo.15587122).

Acknowledgements

We thank Dr. Deyu Xie (NC State University, USA) for generously sharing an aliquot of ascorbic acid with us to run the experimental validation of this work. Generative Artificial Intelligence (Open AI) was utilized to assist in the troubleshooting of writing the RStudio scripts utilized to analyze statistically and plot the results.

Author contributions

M.F., V.A.-S., M.A.B., N.S., ANS, and JMA designed the research. D.A. generated the *vtc2/OE-VTC2* line in N.S.'s laboratory, M.F. designed and performed the experiments, C.M-P. extracted RNA for RNA-seq, assembled the first transcriptome, and analyzed the data. M.F., V.Z., J.M.-C., and I.M. curated and analyzed the data. M.F. and V.Z. generated and curated the R scripts necessary to run correlation analyses and for the visualization of the results. M.F. and V.A.-S. wrote the manuscript with the contribution of all other authors.

Funding

M.F. was supported by the Spanish Ministerio de Educación, Cultura y Deporte para la Formación del Profesorado Universitario (FPU014/01974) and the National Science Foundation grants 1444561 and 1750006. V.A.-S. was funded by a grant ("Programa Emergia 2023", DGP_EMEC_2023_00375) by "Consejería de Universidad, Investigación e Innovación de la Junta de Andalucía". N.S. funded by the Biotechnology and Biological Sciences Research Council (BB/N001311/1). C.M.-P. was funded by Junta de Andalucía (UMA20-FEDERJA-093 and Postdoctoral program, POSTDOC_21_00893). Auxin work in the A.N.S and J.M.A labs was supported by the National Science Foundation grants 1444561 to JMA and ANS, and 1750006 to ANS, and Research Capacity Fund (HATCH) project awards 7005468 and 7005482 from the U.S. Department of Agriculture's National Institute of Food and Agriculture to JMA and ANS, respectively. Funding for open access charge: Universidad de Málaga/CBUA.

References

Aarabi F, Ghigi A, Ahchige MW, Bulut M, Geigenberger P, Neuhaus HE, Sampathkumar A, Alseekh S, Fernie AR (2023) Genome-wide association study unveils ascorbate regulation by PAS/LOV PROTEIN during high light acclimation. Plant Physiol **193**: 2037–2054

Ahmad Z, Ramakrishnan M, Wang C, Rehman S, Shahzad A, Wei Q (2024) Unravelling the role of WRKY transcription factors in leaf senescence: Genetic and molecular insights. J Adv Res. doi: 10.1016/j.jare.2024.09.026

Akram NA, Shafiq F, Ashraf M (2017) Ascorbic Acid-A Potential Oxidant Scavenger and Its Role in Plant Development and Abiotic Stress Tolerance. Front Plant Sci **8**: 613

Andrade Galan AG, Doll J, von Roepenack-Lahaye E, Faiss N, Zentgraf U (2025) The transcription factor WRKY25 can act as redox switch to drive the expression of WRKY53 during leaf senescence in arabidopsis. Sci Rep **15**: 27623

Arnaud D, Deeks MJ, Smirnoff N (2022) Organelle-targeted biosensors reveal distinct oxidative events during pattern-triggered immune responses. Plant Physiol **191**: 2551–2569

Baldet P, Mori K, Decros G, Beauvoit B, Colombié S, Prigent S, Pétriacq P, Gibon Y (2024) Multi-regulated GDP-l-galactose phosphorylase calls the tune in ascorbate biosynthesis. J Exp Bot **75**: 2631–2643

Barth C, Moeder W, Klessig DF, Conklin PL (2004) The Timing of Senescence and Response to Pathogens Is Altered in the Ascorbate-Deficient Arabidopsis Mutant vitamin c-1. Plant Physiol **134**: 1784–1792

Bengtsson H (2025) R.utils: Various Programming Utilities.

Bennett MJ, Marchant A, Green HG, May ST, Ward SP, Millner PA, Walker AR, Schulz B, Feldmann KA (1996) Arabidopsis AUX1 gene: a permease-like regulator of root gravitropism. Science **273**: 948–950

Bian Z, Gao H, Wang C (2020) NAC Transcription Factors as Positive or Negative Regulators during Ongoing Battle between Pathogens and Our Food Crops. Int J Mol Sci **22**: 81

Birkenbihl RP, Kracher B, Roccaro M, Somssich IE (2017) Induced Genome-Wide Binding of Three Arabidopsis WRKY Transcription Factors during Early MAMP-Triggered Immunity. Plant Cell **29**: 20–38

Blaschke K, Ebata KT, Karimi MM, Zepeda-Martínez JA, Goyal P, Mahapatra S, Tam A, Laird DJ, Hirst M, Rao A, et al (2013) Vitamin C induces Tet-dependent DNA demethylation and a blastocyst-like state in ES cells. Nature **500**: 222–226

Bolger AM, Lohse M, Usadel B (2014) Trimmomatic: a flexible trimmer for Illumina sequence data. Bioinforma Oxf Engl **30**: 2114–2120

Bournonville C, Mori K, Deslous P, Decros G, Blomeier T, Mauxion J-P, Jorly J, Gadin S, Cassan C, Maucourt M, et al (2023) Blue light promotes ascorbate synthesis by deactivating the PAS/LOV photoreceptor that inhibits GDP-L-galactose phosphorylase. Plant Cell **35**: 2615–2634

Brumos J, Robles LM, Yun J, Vu TC, Jackson S, Alonso JM, Stepanova AN (2018) Local Auxin Biosynthesis Is a Key Regulator of Plant Development. Dev Cell **47**: 306-318.e5

Brumos J, Zhao C, Gong Y, Soriano D, Patel AP, Perez-Amador MA, Stepanova AN, Alonso JM (2020) An Improved Recombineering Toolset for Plants. Plant Cell **32**: 100–122

Bulley SM, Cooney JM, Laing W (2021) Elevating Ascorbate in Arabidopsis Stimulates the Production of Abscisic Acid, Phaseic Acid, and to a Lesser Extent Auxin (IAA) and Jasmonates, Resulting in Increased Expression of DHAR1 and Multiple Transcription Factors Associated with Abiotic Stress Tolerance. Int J Mol Sci **22**: 6743

Bulley SM, Rassam M, Hoser D, Otto W, Schünemann N, Wright M, MacRae E, Gleave A, Laing W (2009) Gene expression studies in kiwifruit and gene over-expression in Arabidopsis indicates that GDP-L-galactose guanyltransferase is a major control point of vitamin C biosynthesis. J Exp Bot **60**: 765–778

Carril P, da Silva AB, Tenreiro R, Cruz C (2020) An Optimized in situ Quantification Method of Leaf H2O2 Unveils Interaction Dynamics of Pathogenic and Beneficial Bacteria in Wheat. Front Plant Sci. doi: 10.3389/fpls.2020.00889

Champely S, Ekstrom C, Dalgaard P, Gill J, Weibelzahl S, Anandkumar A, Ford C, Volcic R, Rosario HD (2020) pwr: Basic Functions for Power Analysis.

Chatterjee IB (1973) Evolution and the biosynthesis of ascorbic acid. Science **182**: 1271–1272

Chen M, Dai Y, Liao J, Wu H, Lv Q, Huang Y, Liu L, Feng Y, Lv H, Zhou B, et al (2024) TARGET OF MONOPTEROS: key transcription factors orchestrating plant development and environmental response. J Exp Bot **75**: 2214–2234

Chen X, Li C, Wang H, Guo Z (2019) WRKY transcription factors: evolution, binding, and action. Phytopathol Res **1**: 13

Clough SJ, Bent AF (1998) Floral dip: a simplified method for -mediated transformation of. Plant J **16**: 735–743

Conklin PL, DePaolo D, Wintle B, Schatz C, Buckenmeyer G (2013) Identification of Arabidopsis VTC3 as a putative and unique dual function protein kinase::protein phosphatase involved in the regulation of the ascorbic acid pool in plants. J Exp Bot **64**: 2793–2804

Daudi A, O'Brien JA (2012) Detection of Hydrogen Peroxide by DAB Staining in Arabidopsis Leaves. Bio-Protoc **2**: e263

Davuluri RV, Sun H, Palaniswamy SK, Matthews N, Molina C, Kurtz M, Grotewold E (2003) AGRIS: Arabidopsis gene regulatory information server, an information resource of Arabidopsis cis-regulatory elements and transcription factors. BMC Bioinformatics **4**: 25

Daxinger L, Hunter B, Sheikh M, Jauvion V, Gasciolli V, Vaucheret H, Matzke M, Furner I (2008) Unexpected silencing effects from T-DNA tags in Arabidopsis. Trends Plant Sci **13**: 4–6

Delarue M, Prinsen E, Va H, Onckelen, Caboche M, Bellini C (1998) Sur2 mutations of Arabidopsis thaliana define a new locus involved in the control of auxin homeostasis. Plant J **14**: 603–611

Dinno A (2024) dunn.test: Dunn's Test of Multiple Comparisons Using Rank Sums.

Dowdle J, Ishikawa T, Gatzek S, Rolinski S, Smirnoff N (2007) Two genes in Arabidopsis thaliana encoding GDP-L-galactose phosphorylase are required for ascorbate biosynthesis and seedling viability. Plant J Cell Mol Biol **52**: 673–689

Drechsler T, Li Z, Schulze WX, Harter K (2025) Phosphoproteomics uncovers rapid and specific transition from plant two-component system signaling to Ser/Thr phosphorylation by the intracellular redox sensor AHK5. 2025.10.13.682113

Edgar R, Domrachev M, Lash AE (2002) Gene Expression Omnibus: NCBI gene expression and hybridization array data repository. Nucleic Acids Res **30**: 207–210

Endres S, Tenhaken R (2009) Myoinositol oxygenase controls the level of myoinositol in Arabidopsis, but does not increase ascorbic acid. Plant Physiol **149**: 1042–1049

Endrizzi K, Moussian B, Haecker A, Levin JZ, Laux T (1996) The SHOOT MERISTEMLESS gene is required for maintenance of undifferentiated cells in Arabidopsis shoot and floral meristems and acts at a different regulatory level than the meristem genes WUSCHEL and ZWILLE. Plant J Cell Mol Biol **10**: 967–979

Fenech M, Amaya I, Valpuesta V, Botella MA (2019) Vitamin C Content in Fruits: Biosynthesis and Regulation. Front Plant Sci. doi: 10.3389/fpls.2018.02006

Fenech M, Amorim-Silva V, Esteban Del Valle A, Arnaud D, Ruiz-Lopez N, Castillo AG, Smirnoff N, Botella MA (2021) The role of GDP-l-galactose phosphorylase in the control of ascorbate biosynthesis. Plant Physiol **185**: 1574–1594

Fenech M, Brumos J, Pěnčík A, Edwards B, Belcapo S, DeLacey J, Patel A, Kater MM, Li X, Ljung K, et al (2025) The CYP71A, NIT, AMI, and IAMH gene families are dispensable for indole-3-acetaldoxime-mediated auxin biosynthesis in Arabidopsis. Plant Cell koaf242

Fichman Y, Zandalinas SI, Peck S, Luan S, Mittler R (2022) HPCA1 is required for systemic reactive oxygen species and calcium cell-to-cell signaling and plant acclimation to stress. Plant Cell **34**: 4453–4471

Footitt S, Walley PG, Lynn JR, Hambidge AJ, Penfield S, Finch-Savage WE (2020) Trait analysis reveals DOG1 determines initial depth of seed dormancy, but not changes

during dormancy cycling that result in seedling emergence timing. New Phytol **225**: 2035–2047

Fox J, Weisberg S (2019) An R Companion to Applied Regression, Third. Sage, Thousand Oaks, CA

Foyer CH, Kunert K (2024) The ascorbate–glutathione cycle coming of age. J Exp Bot **75**: 2682–2699

Gao Q, Zhang L (2008) Ultraviolet-B-induced oxidative stress and antioxidant defense system responses in ascorbate-deficient vtc1 mutants of Arabidopsis thaliana. J Plant Physiol **165**: 138–148

Gao Y, Nishikawa H, Badejo AA, Shibata H, Sawa Y, Nakagawa T, Maruta T, Shigeoka S, Smirnoff N, Ishikawa T (2011) Expression of aspartyl protease and C3HC4-type RING zinc finger genes are responsive to ascorbic acid in Arabidopsis thaliana. J Exp Bot **62**: 3647–3657

Garnier S, Ross N, Rudis B, Sciaini M, Camargo AP, Scherer C (2024) viridis: Colorblind-Friendly Color Maps for R.

Gautrat P, Buti S, Romanowski A, Lammers M, Matton SEA, Buijs G, Pierik R (2024) Phytochrome-dependent responsiveness to root-derived cytokinins enables coordinated elongation responses to combined light and nitrate cues. Nat Commun **15**: 8489

Ge SX, Son EW, Yao R (2018) iDEP: an integrated web application for differential expression and pathway analysis of RNA-Seq data. BMC Bioinformatics **19**: 534

Goff L, Trapnell C, Kelley D (2014) cummeRbund: Analysis, exploration, manipulation, and visualization of Cufflinks high-throughput sequencing data.

Graeber K, Linkies A, Steinbrecher T, Mummenhoff K, Tarkowská D, Turečková V, Ignatz M, Sperber K, Voegele A, de Jong H, et al (2014) DELAY OF GERMINATION 1 mediates a conserved coat-dormancy mechanism for the temperature- and gibberellin-dependent control of seed germination. Proc Natl Acad Sci **111**: E3571–E3580

Grau J, Franco-Zorrilla JM (2022) TDTHub, a web server tool for the analysis of transcription factor binding sites in plants. Plant J Cell Mol Biol **111**: 1203–1215

Graves S, Dorai-Raj H-PP and LS with help from S (2024) multcompView: Visualizations of Paired Comparisons.

Gu Z (2022) Complex heatmap visualization. iMeta **1**: e43

Gu Z, Eils R, Schlesner M (2016) Complex heatmaps reveal patterns and correlations in multidimensional genomic data. Bioinformatics **32**: 2847–2849

Heberle H, Meirelles GV, da Silva FR, Telles GP, Minghim R (2015) InteractiVenn: a web-based tool for the analysis of sets through Venn diagrams. BMC Bioinformatics **16**: 169

Hoang MTT, Doan MTA, Nguyen T, Tra D-P, Chu TN, Dang TPT, Quach PND (2021) Phenotypic Characterization of Arabidopsis Ascorbate and Glutathione Deficient Mutants under Abiotic Stresses. Agronomy **11**: 764

Horemans N, Asard H, Caubergs RJ (1998) Carrier mediated uptake of dehydroascorbate into higher plant plasma membrane vesicles shows trans-stimulation. FEBS Lett **421**: 41–44

Horemans N, Foyer CH, Asard H (2000) Transport and action of ascorbate at the plant plasma membrane. Trends Plant Sci **5**: 263–267

Horemans N, Szarka A, De Bock M, Raeymaekers T, Potters G, Levine M, Banhégyi G, Guisez Y (2008) Dehydroascorbate and glucose are taken up into Arabidopsis thaliana cell cultures by two distinct mechanisms. FEBS Lett **582**: 2714–2718

Horikoshi M, Tang [aut Y, cre, Dickey A, Grenié M, Thompson R, Selzer L, Strbenac D, Voronin K, Pulatov D (2024) ggfortify: Data Visualization Tools for Statistical Analysis Results.

Hu L, Lu J, Cheng J, Rao Q, Li Z, Hou H, Lou Z, Zhang L, Li W, Gong W, et al (2015) Structural insight into substrate preference for TET-mediated oxidation. Nature **527**: 118–122

Hu Y, Dong Q, Yu D (2012) *Arabidopsis* WRKY46 coordinates with WRKY70 and WRKY53 in basal resistance against pathogen *Pseudomonas syringae*. Plant Sci **185–186**: 288–297

Huang C, He W, Guo J, Chang X, Su P, Zhang L (2005) Increased sensitivity to salt stress in an ascorbate-deficient Arabidopsis mutant. J Exp Bot **56**: 3041–3049

Jiang K, Meng YL, Feldman LJ (2003) Quiescent center formation in maize roots is associated with an auxin-regulated oxidizing environment. Dev Camb Engl **130**: 1429–1438

Joo JH, Bae YS, Lee JS (2001) Role of Auxin-Induced Reactive Oxygen Species in Root Gravitropism. Plant Physiol **126**: 1055–1060

Kakan X, Yu Y, Li S, Li X, Huang R, Wang J (2021) Ascorbic acid modulation by ABI4 transcriptional repression of VTC2 in the salt tolerance of Arabidopsis. BMC Plant Biol **21**: 112

Kassambara A (2023a) ggpubr: "ggplot2" Based Publication Ready Plots.

Kassambara A (2023b) rstatix: Pipe-Friendly Framework for Basic Statistical Tests.

Kawade K, Horiguchi G, Tsukaya H (2010) Non-cell-autonomously coordinated organ size regulation in leaf development. Dev Camb Engl **137**: 4221–4227

Kay M, Elkin LA, Higgins JJ, Wobbrock JO (2025) ARTool: Aligned Rank Transform for Nonparametric Factorial ANOVAs.

Kerchev PI, Pellny TK, Vivancos PD, Kiddle G, Hedden P, Driscoll S, Vanacker H, Verrier P, Hancock RD, Foyer CH (2011) The transcription factor ABI4 Is required for the

ascorbic acid-dependent regulation of growth and regulation of jasmonate-dependent defense signaling pathways in Arabidopsis. Plant Cell **23**: 3319–3334

Kerk NM, Jiang K, Feldman LJ (2000) Auxin Metabolism in the Root Apical Meristem. Plant Physiol **122**: 925–932

Kim BC, Soh MS, Kang BJ, Furuya M, Nam HG (1996) Two dominant photomorphogenic mutations of Arabidopsis thaliana identified as suppressor mutations of hy2. Plant J **9**: 441–456

Kim D, Langmead B, Salzberg SL (2015) HISAT: a fast spliced aligner with low memory requirements. Nat Methods **12**: 357–360

Korbei B, Moulinier-Anzola J, De-Araujo L, Lucyshyn D, Retzer K, Khan MA, Luschnig C (2013) *Arabidopsis* TOL Proteins Act as Gatekeepers for Vacuolar Sorting of PIN2 Plasma Membrane Protein. Curr Biol **23**: 2500–2505

Krishnamurthy A, Rathinasabapathi B (2013) Oxidative stress tolerance in plants. Plant Signal Behav **8**: e25761

Krüger T, Brandt D, Sodenkamp J, Gasper M, Romera-Branchat M, Ahloumessou F, Gehring E, Drotleff J, Bell C, Kramer K, et al (2025) DOG1 controls dormancy independently of ABA core signaling kinases regulation by preventing AFP dephosphorylation through AHG1. Sci Adv **11**: eadr8502

Kubalová M, Müller K, Dobrev PI, Rizza A, Jones AM, Fendrych M (2024) Auxin co-receptor IAA17/AXR3 controls cell elongation in Arabidopsis thaliana root solely by modulation of nuclear auxin pathway. New Phytol **241**: 2448–2463

Laing WA, Martínez-Sánchez M, Wright MA, Bulley SM, Brewster D, Dare AP, Rassam M, Wang D, Storey R, Macknight RC, et al (2015) An upstream open reading frame is essential for feedback regulation of ascorbate biosynthesis in Arabidopsis. Plant Cell **27**: 772–786

Lavenus J, Goh T, Roberts I, Guyomarc'h S, Lucas M, De Smet I, Fukaki H, Beeckman T, Bennett M, Laplaze L (2013) Lateral root development in Arabidopsis: fifty shades of auxin. Trends Plant Sci **18**: 450–458

Lee Y, Kim MW, Kim SH (2007) Cell type identity inArabidopsis roots is altered by both ascorbic acid-induced changes in the redox environment and the resultant endogenous auxin response. J Plant Biol **50**: 484–489

Lee Y, Park CH, Ram Kim A, Chang SC, Kim S-H, Lee WS, Kim S-K (2011) The effect of ascorbic acid and dehydroascorbic acid on the root gravitropic response in Arabidopsis thaliana. Plant Physiol Biochem PPB **49**: 909–916

Leyser HM, Pickett FB, Dharmasiri S, Estelle M (1996) Mutations in the AXR3 gene of Arabidopsis result in altered auxin response including ectopic expression from the SAUR-AC1 promoter. Plant J Cell Mol Biol **10**: 403–413

Liao S, Li K, Wei Y, Zhao S, Zhang M, Wang J, Jiang J, Chen T, Wu F, Fan J, et al (2025) Nucleobase-ascorbate transporter OsNAT9 regulates seed vigor and drought tolerance by modulating ascorbic acid homeostasis in rice. Plant J Cell Mol Biol **122**: e70225

Lim B, Smirnoff N, Cobbett CS, Golz JF (2016) Ascorbate-Deficient vtc2 Mutants in Arabidopsis Do Not Exhibit Decreased Growth. Front Plant Sci **7**: 1025

Linster CL, Gomez TA, Christensen KC, Adler LN, Young BD, Brenner C, Clarke SG (2007) Arabidopsis VTC2 encodes a GDP-L-galactose phosphorylase, the last unknown enzyme in the Smirnoff-Wheeler pathway to ascorbic acid in plants. J Biol Chem **282**: 18879–18885

Lipner S (2018) A classic case of scurvy. Lancet Lond Engl **392**: 431

Liscum E, Askinosie SK, Leuchtman DL, Morrow J, Willenburg KT, Coats DR (2014) Phototropism: Growing towards an Understanding of Plant Movement[OPEN]. Plant Cell **26**: 38–55

Liu S, Kracher B, Ziegler J, Birkenbihl RP, Somssich IE (2015) Negative regulation of ABA signaling by WRKY33 is critical for Arabidopsis immunity towards Botrytis cinerea 2100. eLife **4**: e07295

Lorence A, Chevone BI, Mendes P, Nessler CL (2004) myo-inositol oxygenase offers a possible entry point into plant ascorbate biosynthesis. Plant Physiol **134**: 1200–1205

Lukowitz W, Nickle TC, Meinke DW, Last RL, Conklin PL, Somerville CR (2001) Arabidopsis cyt1 mutants are deficient in a mannose-1-phosphate guanylyltransferase and point to a requirement of N-linked glycosylation for cellulose biosynthesis. Proc Natl Acad Sci U S A **98**: 2262–2267

Mangano S, Denita-Juarez SP, Choi H-S, Marzol E, Hwang Y, Ranocha P, Velasquez SM, Borassi C, Barberini ML, Aptekmann AA, et al (2017) Molecular link between auxin and ROS-mediated polar growth. Proc Natl Acad Sci U S A **114**: 5289–5294

Marchant A, Bhalerao R, Casimiro I, Eklöf J, Casero PJ, Bennett M, Sandberg G (2002) AUX1 promotes lateral root formation by facilitating indole-3-acetic acid distribution between sink and source tissues in the Arabidopsis seedling. Plant Cell **14**: 589–597

Marchant A, Kargul J, May ST, Muller P, Delbarre A, Perrot-Rechenmann C, Bennett MJ (1999) AUX1 regulates root gravitropism in Arabidopsis by facilitating auxin uptake within root apical tissues. EMBO J **18**: 2066–2073

Mellidou I, Kanellis AK (2024) Revisiting the role of ascorbate oxidase in plant systems. J Exp Bot **75**: 2740–2753

Mi H, Muruganujan A, Huang X, Ebert D, Mills C, Guo X, Thomas PD (2019) Protocol Update for large-scale genome and gene function analysis with the PANTHER classification system (v.14.0). Nat Protoc **14**: 703–721

Milne I, Stephen G, Bayer M, Cock PJA, Pritchard L, Cardle L, Shaw PD, Marshall D (2013) Using Tablet for visual exploration of second-generation sequencing data. Brief Bioinform **14**: 193–202

Minor EA, Court BL, Young JI, Wang G (2013) Ascorbate induces ten-eleven translocation (Tet) methylcytosine dioxygenase-mediated generation of 5-hydroxymethylcytosine. J Biol Chem **288**: 13669–13674

Mlotshwa S, Pruss GJ, Gao Z, Mgutshini NL, Li J, Chen X, Bowman LH, Vance V (2010) Transcriptional Silencing Induced by Arabidopsis T-DNA Mutants is Associated with 35S Promoter siRNAs and Requires Genes Involved in siRNA-mediated Chromatin Silencing. Plant J Cell Mol Biol **64**: 699–704

Mounet-Gilbert L, Dumont M, Ferrand C, Bournonville C, Monier A, Jorly J, Lemaire-Chamley M, Mori K, Atienza I, Hernould M, et al (2016) Two tomato GDP-D-mannose epimerase isoforms involved in ascorbate biosynthesis play specific roles in cell wall biosynthesis and development. J Exp Bot **67**: 4767–4777

Mukherjee M, Larrimore KE, Ahmed NJ, Bedick TS, Barghouthi NT, Traw MB, Barth C (2010) Ascorbic acid deficiency in arabidopsis induces constitutive priming that is dependent on hydrogen peroxide, salicylic acid, and the NPR1 gene. Mol Plant-Microbe Interact MPMI **23**: 340–351

Nakagawa T, Kurose T, Hino T, Tanaka K, Kawamukai M, Niwa Y, Toyooka K, Matsuoka K, Jinbo T, Kimura T (2007) Development of series of gateway binary vectors, pGWBs, for realizing efficient construction of fusion genes for plant transformation. J Biosci Bioeng **104**: 34–41

Neuteboom LW, Ng JM, Kuyper M, Clijdesdale OR, Hooykaas PJ, van der Zaal BJ (1999) Isolation and characterization of cDNA clones corresponding with mRNAs that accumulate during auxin-induced lateral root formation. Plant Mol Biol **39**: 273–287

Nguyen NH, Sng BJR, Chin HJ, Choi IKY, Yeo HC, Jang I-C (2023) HISTONE DEACETYLASE 9 promotes hypocotyl-specific auxin response under shade. Plant J **116**: 804–822

Norris SR, Shen X, Della Penna D (1998) Complementation of the Arabidopsis pds1 Mutation with the Gene Encoding p-Hydroxyphenylpyruvate Dioxygenase. Plant Physiol **117**: 1317–1323

O'Malley RC, Huang S-SC, Song L, Lewsey MG, Bartlett A, Nery JR, Galli M, Gallavotti A, Ecker JR (2016) Cistrome and Epicistrome Features Shape the Regulatory DNA Landscape. Cell **165**: 1280–1292

Padayatty SJ, Levine M (2016) Vitamin C: the known and the unknown and Goldilocks. Oral Dis **22**: 463–493

Page M, Sultana N, Paszkiewicz K, Florance H, Smirnoff N (2012) The influence of ascorbate on anthocyanin accumulation during high light acclimation in Arabidopsis thaliana: further evidence for redox control of anthocyanin synthesis. Plant Cell Environ **35**: 388–404

Palaniswamy SK, James S, Sun H, Lamb RS, Davuluri RV, Grotewold E (2006) AGRIS and AtRegNet. a platform to link cis-regulatory elements and transcription factors into regulatory networks. Plant Physiol **140**: 818–829

Pasternak T, Palme K, Pérez-Pérez JM (2023) Role of reactive oxygen species in the modulation of auxin flux and root development in Arabidopsis thaliana. Plant J Cell Mol Biol **114**: 83–95

Pastor V, Luna E, Ton J, Cerezo M, García-Agustín P, Flors V (2013) Fine tuning of reactive oxygen species homeostasis regulates primed immune responses in Arabidopsis. Mol Plant-Microbe Interact MPMI **26**: 1334–1344

Pastori GM, Kiddle G, Antoniw J, Bernard S, Veljovic-Jovanovic S, Verrier PJ, Noctor G, Foyer CH (2003) Leaf Vitamin C Contents Modulate Plant Defense Transcripts and Regulate Genes That Control Development through Hormone Signaling. Plant Cell **15**: 939–951

Pavet V, Olmos E, Kiddle G, Mowla S, Kumar S, Antoniw J, Alvarez ME, Foyer CH (2005) Ascorbic acid deficiency activates cell death and disease resistance responses in Arabidopsis. Plant Physiol **139**: 1291–1303

Peer WA, Cheng Y, Murphy AS (2013) Evidence of oxidative attenuation of auxin signalling. J Exp Bot **64**: 2629–2639

Pignocchi C, Foyer CH (2003) Apoplastic ascorbate metabolism and its role in the regulation of cell signalling. Curr Opin Plant Biol **6**: 379–389

Pineau B, Layoune O, Danon A, De Paepe R (2008) l-Galactono-1,4-lactone Dehydrogenase Is Required for the Accumulation of Plant Respiratory Complex I*. J Biol Chem **283**: 32500–32505

de Pinto MC, De Gara L (2004) Changes in the ascorbate metabolism of apoplastic and symplastic spaces are associated with cell differentiation. J Exp Bot **55**: 2559–2569

Qi T, Liu Z, Fan M, Chen Y, Tian H, Wu D, Gao H, Ren C, Song S, Xie D (2017) GDP-D-mannose epimerase regulates male gametophyte development, plant growth and leaf senescence in Arabidopsis. Sci Rep **7**: 10309

Qin C, Qian W, Wang W, Wu Y, Yu C, Jiang X, Wang D, Wu P (2008) GDP-mannose pyrophosphorylase is a genetic determinant of ammonium sensitivity in Arabidopsis thaliana. Proc Natl Acad Sci U S A **105**: 18308–18313

R Core Team (2025) R: A Language and Environment for Statistical Computing.

Ran X, Zhao F, Wang Y, Liu J, Zhuang Y, Ye L, Qi M, Cheng J, Zhang Y (2020) Plant Regulomics: a data-driven interface for retrieving upstream regulators from plant multi-omics data. Plant J **101**: 237–248

Reikersdorfer KN, Singh A, Young JD, Batty MB, Steele AE, Yuen LC, Momtaz DA, Weissert JN, Liu DS, Hogue GD (2024) The Troubling Rise of Scurvy: A Review and

National Analysis of Incidence, Associated Risk Factors, and Clinical Manifestations. J Am Acad Orthop Surg Glob Res Rev **8**: e24.00162

Reuber TL, Ausubel FM (1996) Isolation of Arabidopsis genes that differentiate between resistance responses mediated by the RPS2 and RPM1 disease resistance genes. Plant Cell **8**: 241–249

Romano CP, Robson PR, Smith H, Estelle M, Klee H (1995) Transgene-mediated auxin overproduction in Arabidopsis: hypocotyl elongation phenotype and interactions with the hy6-1 hypocotyl elongation and axr1 auxin-resistant mutants. Plant Mol Biol **27**: 1071–1083

Roychoudhry S, Kepinski S (2022) Auxin in Root Development. Cold Spring Harb Perspect Biol **14**: a039933

Schindelin J, Arganda-Carreras I, Frise E, Kaynig V, Longair M, Pietzsch T, Preibisch S, Rueden C, Saalfeld S, Schmid B, et al (2012) Fiji: an open-source platform for biological-image analysis. Nat Methods **9**: 676–682

Schopfer P, Liszkay A, Bechtold M, Frahry G, Wagner A (2002) Evidence that hydroxyl radicals mediate auxin-induced extension growth. Planta **214**: 821–828

Seo PJ, Lee A-K, Xiang F, Park C-M (2008) Molecular and functional profiling of Arabidopsis pathogenesis-related genes: insights into their roles in salt response of seed germination. Plant Cell Physiol **49**: 334–344

Smirnoff N (2018) Ascorbic acid metabolism and functions: A comparison of plants and mammals. Free Radic Biol Med **122**: 116–129

Smirnoff N, Wheeler GL (2024) The ascorbate biosynthesis pathway in plants is known, but there is a way to go with understanding control and functions. J Exp Bot **75**: 2604–2630

Spurney RJ, Van den Broeck L, Clark NM, Fisher AP, de Luis Balaguer MA, Sozzani R (2020) tuxnet: a simple interface to process RNA sequencing data and infer gene regulatory networks. Plant J **101**: 716–730

Stepanova AN, Hoyt JM, Hamilton AA, Alonso JM (2005) A Link between Ethylene and Auxin Uncovered by the Characterization of Two Root-Specific Ethylene-Insensitive Mutants in Arabidopsis. Plant Cell **17**: 2230–2242

Stepanova AN, Robertson-Hoyt J, Yun J, Benavente LM, Xie D-Y, Doležal K, Schlereth A, Jürgens G, Alonso JM (2008) TAA1-Mediated Auxin Biosynthesis Is Essential for Hormone Crosstalk and Plant Development. Cell **133**: 177–191

Stepanova AN, Yun J, Robles LM, Novak O, He W, Guo H, Ljung K, Alonso JM (2011) The *Arabidopsis* YUCCA1 Flavin Monooxygenase Functions in the Indole-3-Pyruvic Acid Branch of Auxin Biosynthesis. Plant Cell **23**: 3961–3973

Swarup R, Bhosale R (2019) Developmental Roles of AUX1/LAX Auxin Influx Carriers in Plants. Front Plant Sci **10**: 1306

Szecowka M, Heise R, Tohge T, Nunes-Nesi A, Vosloh D, Huege J, Feil R, Lunn J, Nikoloski Z, Stitt M, et al (2013) Metabolic Fluxes in an Illuminated Arabidopsis Rosette. Plant Cell **25**: 694–714

Tao Y, Ferrer J-L, Ljung K, Pojer F, Hong F, Long JA, Li L, Moreno JE, Bowman ME, Ivans LJ, et al (2008) Rapid Synthesis of Auxin via a New Tryptophan-Dependent Pathway Is Required for Shade Avoidance in Plants. Cell **133**: 164–176

Thomas PD, Ebert D, Muruganujan A, Mushayahama T, Albou L-P, Mi H (2022) PANTHER: Making genome-scale phylogenetics accessible to all. Protein Sci Publ Protein Soc **31**: 8–22

Thomma BP, Eggermont K, Penninckx IA, Mauch-Mani B, Vogelsang R, Cammue BP, Broekaert WF (1998) Separate jasmonate-dependent and salicylate-dependent defense-response pathways in Arabidopsis are essential for resistance to distinct microbial pathogens. Proc Natl Acad Sci U S A **95**: 15107–15111

Thordal-Christensen H, Zhang Z, Wei Y, Collinge DB (1997) Subcellular localization of H2O2 in plants. H2O2 accumulation in papillae and hypersensitive response during the barley—powdery mildew interaction. Plant J **11**: 1187–1194

Torabinejad J, Donahue JL, Gunesekera BN, Allen-Daniels MJ, Gillaspy GE (2009) VTC4 is a bifunctional enzyme that affects myoinositol and ascorbate biosynthesis in plants. Plant Physiol **150**: 951–961

Tóth SZ, Schansker G, Garab G (2013) The physiological roles and metabolism of ascorbate in chloroplasts. Physiol Plant **148**: 161–175

Trapnell C, Hendrickson DG, Sauvageau M, Goff L, Rinn JL, Pachter L (2013) Differential analysis of gene regulation at transcript resolution with RNA-seq. Nat Biotechnol **31**: 46–53

Trapnell C, Roberts A, Goff L, Pertea G, Kim D, Kelley DR, Pimentel H, Salzberg SL, Rinn JL, Pachter L (2012) Differential gene and transcript expression analysis of RNA-seq experiments with TopHat and Cufflinks. Nat Protoc **7**: 562–578

Tyburski J, Dunajska-Ordak K, Skorupa M, Tretyn A (2012) Role of Ascorbate in the Regulation of the Arabidopsis thaliana Root Growth by Phosphate Availability. J Bot **2012**: 580342

Tyystjärvi E (2008) Photoinhibition of Photosystem II and photodamage of the oxygen evolving manganese cluster. Coord Chem Rev **252**: 361–376

Uknes S, Mauch-Mani B, Moyer M, Potter S, Williams S, Dincher S, Chandler D, Slusarenko A, Ward E, Ryals J (1992) Acquired resistance in Arabidopsis. Plant Cell **4**: 645–656

Ulmasov T, Murfett J, Hagen G, Guilfoyle TJ (1997) Aux/IAA proteins repress expression of reporter genes containing natural and highly active synthetic auxin response elements. Plant Cell **9**: 1963–1971

Urueña-Palacio S, Ferreyro BL, Fernández-Otero LG, Calo PD (2018) Adult scurvy associated with psychiatric disorders and breast feeding. BMJ Case Rep **2018**: bcr2017223686, bcr-2017–223686

Veljović-Jovanović S, Vidović M, Morina F (2017) Ascorbate as a Key Player in Plant Abiotic Stress Response and Tolerance. *In* MA Hossain, S Munné-Bosch, DJ Burritt, P Diaz-Vivancos, M Fujita, A Lorence, eds, Ascorbic Acid Plant Growth Dev. Stress Toler. Springer International Publishing, Cham, pp 47–109

Wang Q, Shi H, Huang R, Ye R, Luo Y, Guo Z, Lu S (2021) AIR12 confers cold tolerance through regulation of the CBF cold response pathway and ascorbate homeostasis. Plant Cell Environ **44**: 1522–1533

Wang Y, Li Y, Rosas-Diaz T, Caceres-Moreno C, Lozano-Duran R, Macho AP (2019) The IMMUNE-ASSOCIATED NUCLEOTIDE-BINDING 9 Protein Is a Regulator of Basal Immunity in Arabidopsis thaliana. Mol Plant-Microbe Interact MPMI **32**: 65–75

Weijers D, Schlereth A, Ehrismann JS, Schwank G, Kientz M, Jürgens G (2006) Auxin triggers transient local signaling for cell specification in Arabidopsis embryogenesis. Dev Cell **10**: 265–270

Whitford R, Fernandez A, Tejos R, Pérez AC, Kleine-Vehn J, Vanneste S, Drozdzecki A, Leitner J, Abas L, Aerts M, et al (2012) GOLVEN Secretory Peptides Regulate Auxin Carrier Turnover during Plant Gravitropic Responses. Dev Cell **22**: 678–685

Wickham H, Chang W, Henry L, Pedersen TL, Takahashi K, Wilke C, Woo K, Yutani H, Dunnington D, Brand T van den, et al (2025a) ggplot2: Create Elegant Data Visualisations Using the Grammar of Graphics.

Wickham H, François R, Henry L, Müller K, Vaughan D, Software P, PBC (2023) dplyr: A Grammar of Data Manipulation.

Wickham H, Henry L, Pedersen TL, Luciani TJ, Decorde M, Lise V, code) TP (Early line dashing, code) DG (Line dashing code and early raster, implementation) YQ (Improved styles; polypath, code) HM (Opacity, et al (2025b) svglite: An “SVG” Graphics Device.

Wu F, Chi Y, Jiang Z, Xu Y, Xie L, Huang F, Wan D, Ni J, Yuan F, Wu X, et al (2020) Hydrogen peroxide sensor HPCA1 is an LRR receptor kinase in Arabidopsis. Nature **578**: 577–581

Wu S-Y, Hou L-L, Zhu J, Wang Y-C, Zheng Y-L, Hou J-Q, Yang Z-N, Lou Y (2023) Ascorbic acid-mediated reactive oxygen species homeostasis modulates the switch from tapetal cell division to cell differentiation in Arabidopsis. Plant Cell **35**: 1474–1495

Yamada M, Greenham K, Prigge MJ, Jensen PJ, Estelle M (2009) The TRANSPORT INHIBITOR RESPONSE2 Gene Is Required for Auxin Synthesis and Diverse Aspects of Plant Development. Plant Physiol **151**: 168–179

Yilmaz A, Mejia-Guerra MK, Kurz K, Liang X, Welch L, Grotewold E (2011) AGRIS: the Arabidopsis Gene Regulatory Information Server, an update. Nucleic Acids Res **39**: D1118-1122

Young JI, Züchner S, Wang G (2015) Regulation of the Epigenome by Vitamin C. Annu Rev Nutr **35**: 545–564

Yu Y, Wang J, Li S, Kakan X, Zhou Y, Miao Y, Wang F, Qin H, Huang R (2019) Ascorbic Acid Integrates the Antagonistic Modulation of Ethylene and Abscisic Acid in the Accumulation of Reactive Oxygen Species. Plant Physiol **179**: 1861–1875

Yuan X, Wang H, Cai J, Li D, Song F (2019) NAC transcription factors in plant immunity. Phytopathol Res **1**: 3

Zhao Y (2018) Essential Roles of Local Auxin Biosynthesis in Plant Development and in Adaptation to Environmental Changes. Annu Rev Plant Biol **69**: 417–435

Zhao Y, Christensen SK, Fankhauser C, Cashman JR, Cohen JD, Weigel D, Chory J (2001) A role for flavin monooxygenase-like enzymes in auxin biosynthesis. Science **291**: 306–309

Zhao Y, Hull AK, Gupta NR, Goss KA, Alonso J, Ecker JR, Normanly J, Chory J, Celenza JL (2002) Trp-dependent auxin biosynthesis in Arabidopsis: involvement of cytochrome P450s CYP79B2 and CYP79B3. Genes Dev **16**: 3100–3112

Zhou Z-Y, Zhang C-G, Wu L, Zhang C-G, Chai J, Wang M, Jha A, Jia P-F, Cui S-J, Yang M, et al (2011) Functional characterization of the CKRC1/TAA1 gene and dissection of hormonal actions in the Arabidopsis root. Plant J Cell Mol Biol **66**: 516–527

Figure Legends

Figure 1. Arabidopsis ascorbate-altered lines do not show a compensatory response of ascorbate biosynthesis-related genes in four-week-old rosettes. A) Ascorbate biosynthesis (Smirnoff-Wheeler) pathway and its convergence with the biosynthesis of cell wall precursors. B) uORF-less *VTC2* overexpression lines accumulate more VTC2 protein than the native promoter line described in Fenech et al., 2021 in one week-old seedlings. C) A range of endogenous ascorbate concentrations (20% to 165% of wild-type (WT) levels) in four Arabidopsis lines employed in this work enables to study the effect of different ascorbate levels on genome-wide gene expression in four-week-old rosettes. We selected line L15 (from now on, *vtc2/OE-VTC2*) because it accumulated a higher amount of VTC2-GFP protein than L16. The biomass utilized to determine ascorbate concentration and for RNA extraction comes from the same samples. D) RNA-seq analysis confirms the loss of *VTC2* and *VTC4* expression in their respective T-DNA knockout mutants and shows that the expression of other ascorbate biosynthesis-related genes remains largely unaffected in four-week-old rosettes. Different letters in panels C and D denote statistically significant differences (One-Way ANOVA, Tukey post-hoc test, α=0.05, n=3). Mean values and standard deviation are represented. Distributions were tested to meet normality (Shapiro–Wilk's test) and homoscedasticity (Levene's test) prior to ANOVA. If not meeting any of these requirements, data was transformed using logarithm and, if meeting the requirements, proceeded to perform ANOVA. Otherwise, Kruskal-Wallis followed by Dunn's post-hoc test were performed. CBB: Coomassie Brilliant Blue; Glc: glucose, Fru: fructose, Man: mannose, Gal: galactose, GalL: galactono-1,4-lactone, Fuc: fucose; PGI: phosphoglucose isomerase; PMI: phosphomannose isomerase; PMM: phosphomannomutase; GMP: GDP-D-mannose pyrophosphorylase (Arabidopsis *VTC1*), GME: GDP-D-mannose-3',5'-isomerase, GGP: GDP-L-galactose phosphorylase (*VTC2* and *VTC5*), GPP: L-galactose-1-phosphate phosphatase (*VTC4*), L-GalDH: L-galactose dehydrogenase, L-GalLDH: L-galactono-1,4-lactone dehydrogenase. FPKM: Fragments Per Kilobase of transcript per Million mapped reads.

Figure 2. Transcriptome profiles of four-week-old Arabidopsis rosettes with altered concentration of endogenous ascorbate compared to WT. A) Numbers of differentially expressed genes (DEGs) identified at False Discovery Rate (FDR)-corrected p-value (q-value) <0.05. B) Analysis of DEG overlap between the three ascorbate-altered lines. C) GO Biological Process terms associated with induced DEGs. D) GO Biological Process terms associated with repressed DEGs. The symbol ∩ in panel B denotes intersection. E) Overlap of differentially expressed TFs between the three ascorbate-altered lines (listed in Supplementary Dataset S4). *bZIP58 (AT1G13600): BASIC LEUCINE-ZIPPER 58, JJJ1 (AT1G74250): DNAJ HEAT SHOCK N-TERMINAL DOMAIN-CONTAINING PROTEIN, ATC3H5*

(AT1G10320): ZINC FINGER C-X8-C-X5-C-X3-H TYPE FAMILY PROTEIN, BORI1 (AT3G02400): BOREALIN RELATED INTERACTOR 1, STM (AT1G62360): SHOOT MERISTEMLESS, AT5G41020: MYB FAMILY TRANSCRIPTION FACTOR, GIF1 (AT5G28640): GRF1-INTERACTING FACTOR 1.

Figure 3. Identification of genes whose expression is correlated with ascorbate concentration in four-week-old rosettes and that are differentially expressed between the most contrasting ascorbate-altered lines, *vtc2* and *vtc2/OE-VTC2*. A,B) Distribution of statistical confidence values for genes positively (A) and negatively (B) correlated with ascorbate concentrations for genes with a False Discovery Rate (FDR)-corrected p-value (q-value) <0.05 cutoff. C, D) Expression profiles of positively correlated genes (PCGs) (C) and negatively correlated genes (NCGs) (D). Heatmap generated with iDEP (Ge et al., 2018). Hierarchical clustering of PCGs and NCGs was calculated by Pearson correlation distances. The Z-score normalization of the expression data (FPKM) was performed by subtracting the average expression value for each gene and dividing it by the standard deviation. E) The six strongest PCGs based on their relative response (RR) calculated as explained in Supplementary Fig. S6. F) The six strongest NCGs based on their relative response (RR) calculated as explained in Supplementary Fig. S6. G) Genes with prominent roles in auxin homeostasis that showed significant correlation with ascorbate concentration. RNA-seq FPKM values (y-axes) vs ascorbate concentrations (x-axes) are plotted. Different letters denote statistically significant differences (One-Way ANOVA, Tukey post-hoc test, α=0.05, n=3). Distributions were tested to meet normality (Shapiro–Wilk's test) and homoscedasticity (Levene's test) prior to ANOVA. If not meeting any of these requirements, data was transformed using logarithm and, if meeting the requirements, proceeded to perform ANOVA. Otherwise, Kruskal-Wallis followed by Dunn's post-hoc test were performed. FPKM: Fragments Per Kilobase of transcript per Million mapped reads, FW: fresh weight; *SQP1: SQUALENE MONOOXYGENASE, AT5G11330: FAD/NAD(P)-BINDING OXIDOREDUCTASE, DOG1: DELAY OF GERMINATION 1, MIOX1; MYO-INOSITOL OXYGENASE 1, MYOB16: MYOSIN BINDING PROTEIN 16, AT2G27420: CYSTEINE PROTEINASES, AIG1: AVRRPT2-INDUCED GENE 1, PR5: PATHOGENESIS-RELATED GENE 5, AT3G15536: Unknown gene, AT5G13320: AVRPPHB SUSCEPTIBLE 3, HSP70-2: HEAT SHOCK 70 PROTEIN, CRK7: CYSTEINE-RICH RECEPTOR-LIKE PROTEIN KINASE 7, TAA1: TRYPTOPHAN AMINOTRANSFERASE OF ARABIDOPSIS 1, IAA17/AXR3: AUXIN RESISTANT 3/INDOLE-3-ACETIC ACID INDUCIBLE 17, TOL4: TOM1-LIKE 4, AIR12: AUXIN-INDUCED IN ROOT CULTURES 12*.

Figure 4. Ascorbate induces the expression of auxin biosynthesis gene *TAA1* and auxin signaling in Arabidopsis in a light-dependent manner. Panels A, B, E, and F show seedlings grown for 5 days under continuous LED light and panels C, D, G, and H show seedlings grown for 3 days in the dark. A, C) Expression of a recombineering genomic DNA construct, *TAA1p:YPet-gTAA1*, in *wei8-2* roots is increased in light- but not dark-grown seedlings germinated in 0.5 mM ascorbate. B, D) Expression of an auxin-inducible reporter, *DR5:GFP,* in WT and *wei8* mutant backgrounds is induced in roots in light- but not dark-grown seedlings germinated in 0.5 mM ascorbate. Scale bar is applicable to all images within a panel. E, F) The length of roots, but not that of hypocotyls, of light-grown WT seedlings germinated in the media supplemented with 0.5 mM ascorbate is reduced to 35% of the untreated seedlings' length, with *wei8* showing ascorbate hypersensitivity in roots (25% of untreated roots' length). Scale bar is applicable to all images within panel E. G, H) The length of WT roots and hypocotyls of dark-grown seedlings exposed to 0.5 mM ascorbate is statistically indistinguishable from that of untreated plants (90%), whereas *wei8* displays a 25% root growth inhibition in ascorbate. Scale bar is applicable to all images within the panel. Different letters in panels F and H denote statistically significant differences between mean values represented as horizontal black bars (One-Way ANOVA, Tukey post-hoc test, α=0.05). Sample size of ascorbate-treated population is indicated below their respective violin plots and, between parentheses, the sample size of control population they were used to normalize against. Distributions were tested to meet normality (Shapiro–Wilk's test) and homoscedasticity (Levene's test) prior to ANOVA. If not meeting any of these requirements, data was transformed using logarithm and, if meeting the requirements, proceeded to perform ANOVA. Otherwise, Kruskal-Wallis followed by Dunn's post-hoc test were performed. For panels A-D, more than 20 roots per genotype and treatment have been scored through experimental repetitions and a representative image was selected. All microscopy images are Z stacks through the root from the cortical to the equatorial plane, except the details shown in panels A and C, that are stacks of 2-5 equatorial planes.

Figure 5. Ascorbate (Asc)-induced auxin biosynthesis in Arabidopsis relies on *TAA1* and *TAR2*. Panels A, C and D show seedlings grown for 5 days under continuous light, and panel B shows seedlings grown for 3 days in the dark. A, B) Auxin-inducible reporter *DR5:GUS* and recombineering-generated translational fusions of *TAA1* and *TAR2* with *GUS* show increased reporter activity upon media supplementation with 0.5mM ascorbate in light- but not dark-grown plants. 1-mm scale bar is applicable to all cotyledon images within the panel, and 100-µm scale bar is applicable to all root images within the panel. C, D) Plants exposed to 0.5mM ascorbate in the media display reduced root growth as compared to root elongation in the absence of ascorbate. *wei8* mutant shows greater sensitivity to 0.5 mM ascorbate than WT, *tar1 tar2-2* and *tar1 tar2-1,* with *tar1 tar2-2* and *tar1 tar2-1* showing intermediate

response between that of *wei8* and WT. Scale bar is applicable to all images within panel C. Different letters in panel D denote statistically significant differences between mean values represented as horizontal black bars(One-Way ANOVA, Tukey post-hoc test, α=0.05). Sample size of ascorbate-treated population is indicated below their respective violin plots and, between parentheses, the sample size of control population they were used to normalize against Distributions were tested to meet normality (Shapiro–Wilk's test) and homoscedasticity (Levene's test) prior to ANOVA. If not meeting any of these requirements, data was transformed using logarithm and, if meeting the requirements, proceeded to perform ANOVA. Otherwise, Kruskal-Wallis followed by Dunn's post-hoc test was performed.

Figure 6. Exogenous auxin (IAA) partially reverts the root hypersensitivity to ascorbate in *wei8*, but not in *aux1*. Seedlings were germinated for 5 days under continuous light. A) Presence of 100 nM IAA in growth media does not inhibit root growth. B) 100 nM IAA enhances the root growth in presence of 0.5 mM ascorbate (Asc), but it does not fully restore *wei8* and *aux1* mutants' primary root growth. C) Representative images of the phenotypes quantified in A and B. Scale bar is applicable to all images within the panel. Different letters denote statistically significant differences between mean values represented as horizontal black bars (One-Way ANOVA, Tukey post-hoc test, α=0.05). Sample size is indicated below their respective violin plots. Distributions were tested to meet normality (Shapiro–Wilk's test) and homoscedasticity (Levene's test) prior to ANOVA. If not meeting any of these requirements, data was transformed using logarithm and, if meeting the requirements, proceeded to perform ANOVA. Otherwise, Kruskal-Wallis followed by Dunn's post-hoc test was performed. IAA: indole-3-acetic acid.

Figure 7. Model scheme integrating our study into the established model of ascorbate-regulated signaling pathway. A) Subcellular model of compartmentalized ascorbate. Ascorbate is oxidized in the apoplast by means of ascorbate oxidase (AO) and ascorbate peroxidase (APX) activities into monodehydroascorbate (MDHA), which quickly disproportionates into DHA spontaneously or by means of MDHA reductase (MDHAR, not shown here), hence neutralizing H_2O_2 derived from oxidase (OX) activities (e.g., NADPH oxidase). Consequently, ascorbate tunes the signaling activity of surface H_2O_2 receptors (R) that are propagated into the nucleus hence adjusting gene expression. In this study, we identified genes whose expression was positively correlated with ascorbate concentration (PCGs, like auxin-related *TRYPTOPHAN AMINOTRANSFERASE OF ARABIDOPSIS 1 (TAA1), Aux/INDOLE ACETIC ACID 17 (IAA17),* or *ROOT MERISTEM GROWTH FACTOR 9 (RGF9)*) or negatively correlated (NCG, like *TOBAMOVIRUS MULTIPLICATION 1-LIKE 4 (TOL4)* or *AUXIN INDUCED IN ROOTS 12 (AIR12)*. Thus, high ascorbate concentration induces auxin biosynthesis and signaling activities. B) Apoplastic reactive oxygen species (ROS) such as

H_2O_2 contribute to the cell expansion by breaking down the polymers that make the cell wall hence loosening it. Therefore, ascorbate-mediated decrease of ROS promotes cell wall stiffening. This signaling is transduced following the scheme in (A), potentially leading to increased auxin biosynthesis and auxin-mediated accumulation of ROS in the cell wall, partially counteracting ascorbate-induced cell wall stiffening. According to our results, not all cells may have the ability to respond this way, and cell-to-cell auxin transport from auxin source cells (with ascorbate-promoted auxin biosynthesis) through AUX1 towards auxin sink cells (that remain to be identified) is required to counteract the effect of increased ascorbate concentration.

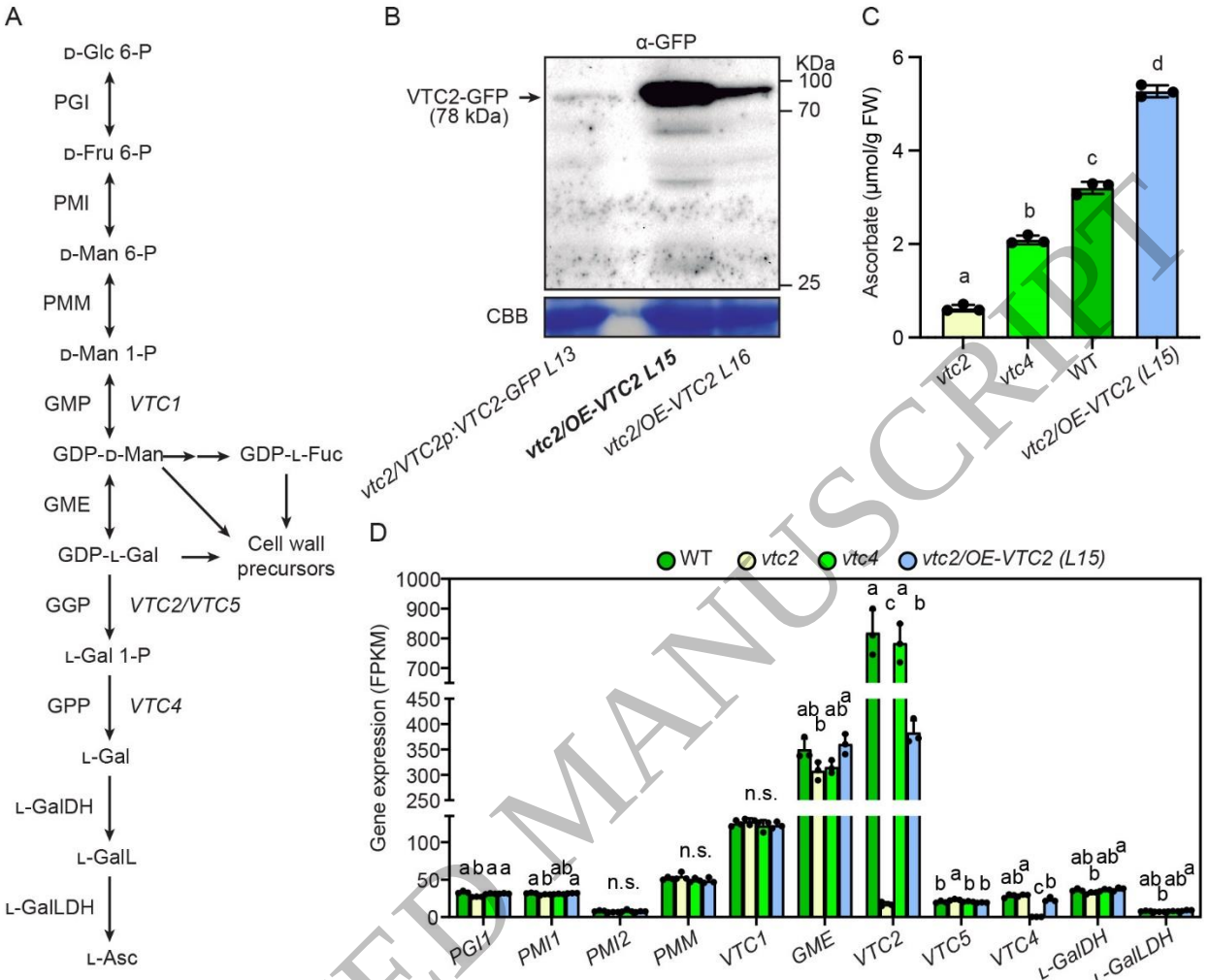

Figure 1
165x138 mm (x DPI)

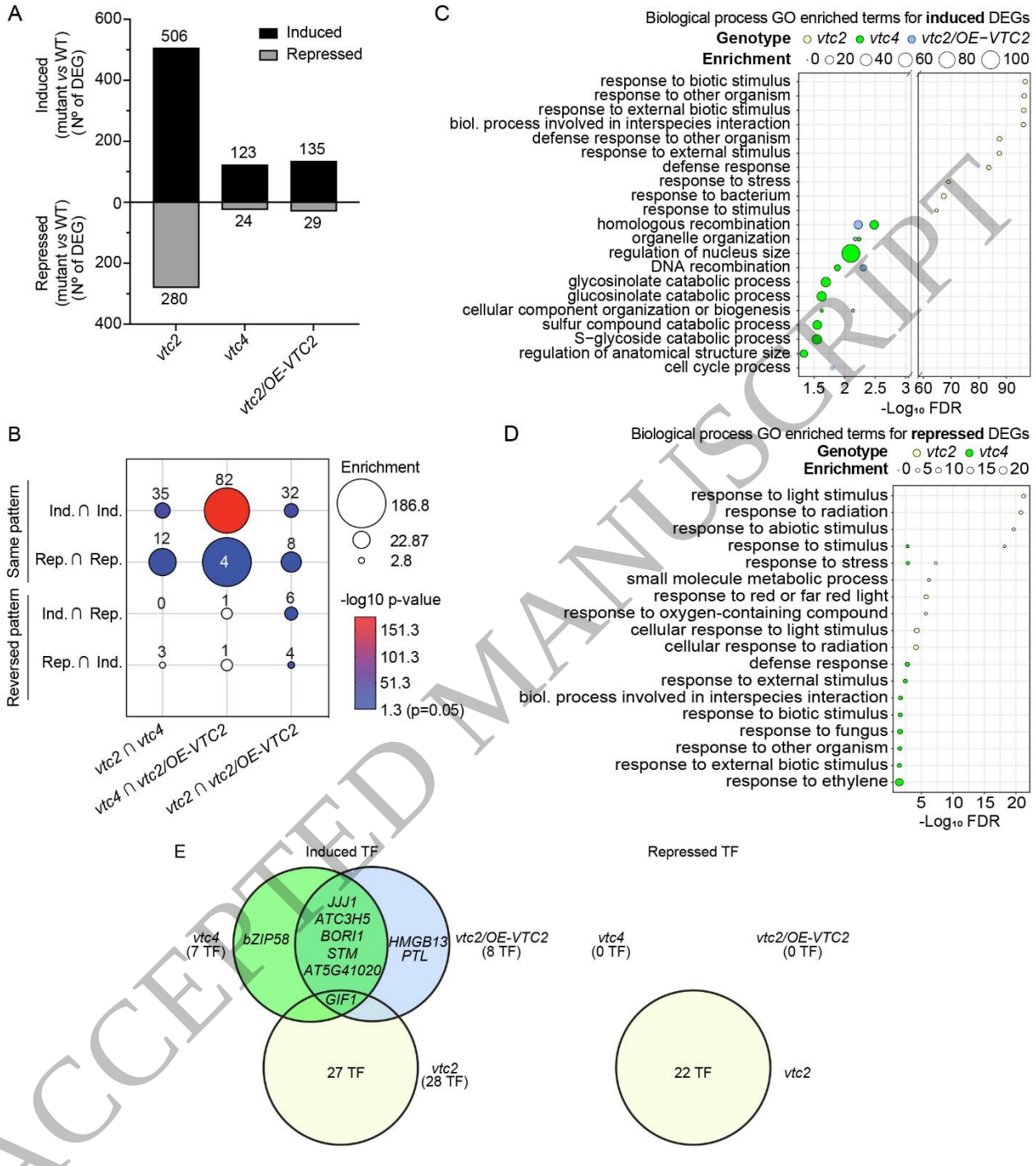

Figure 2
165x183 mm (x DPI)

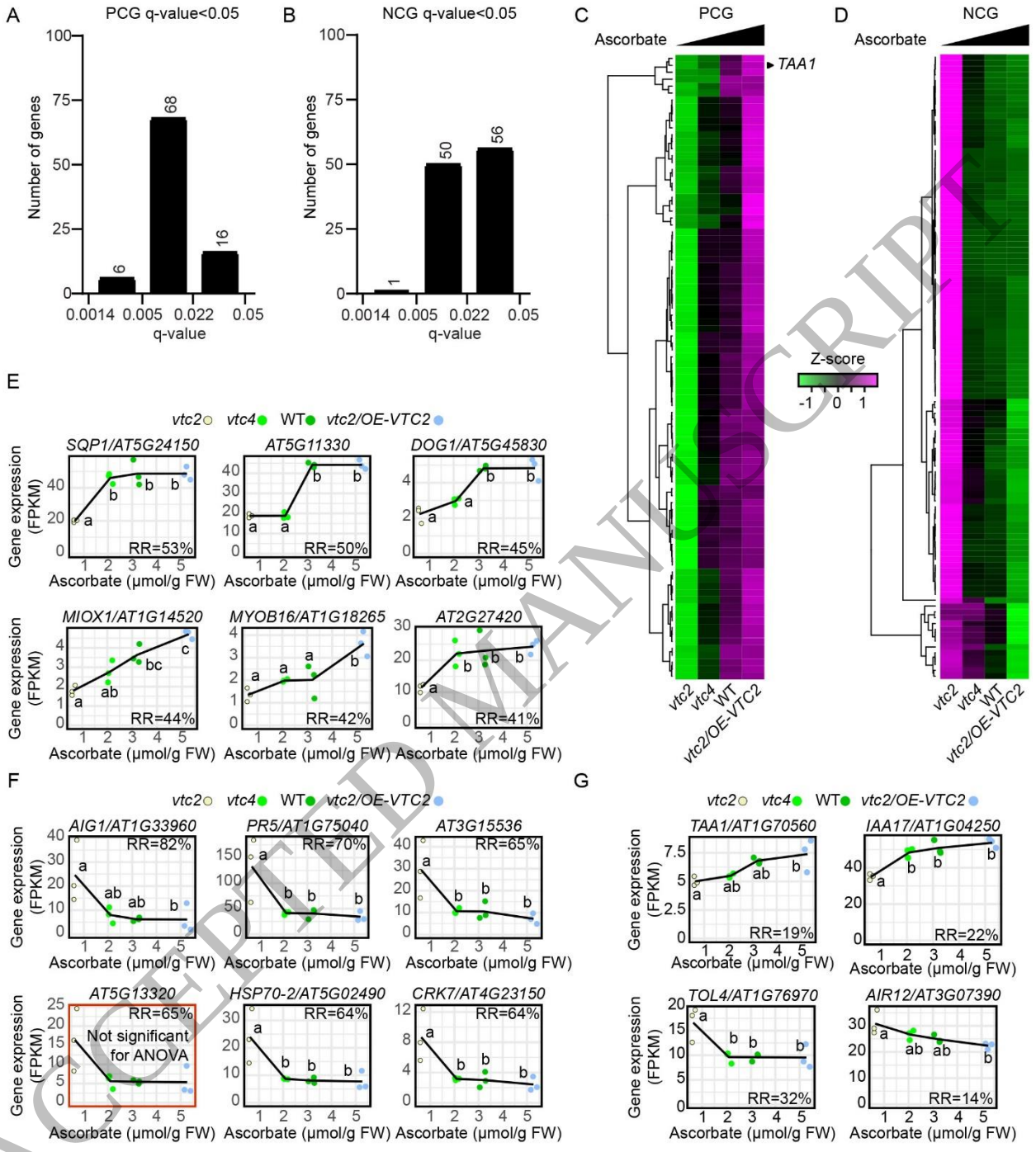

Figure 3
165x183 mm (x DPI)

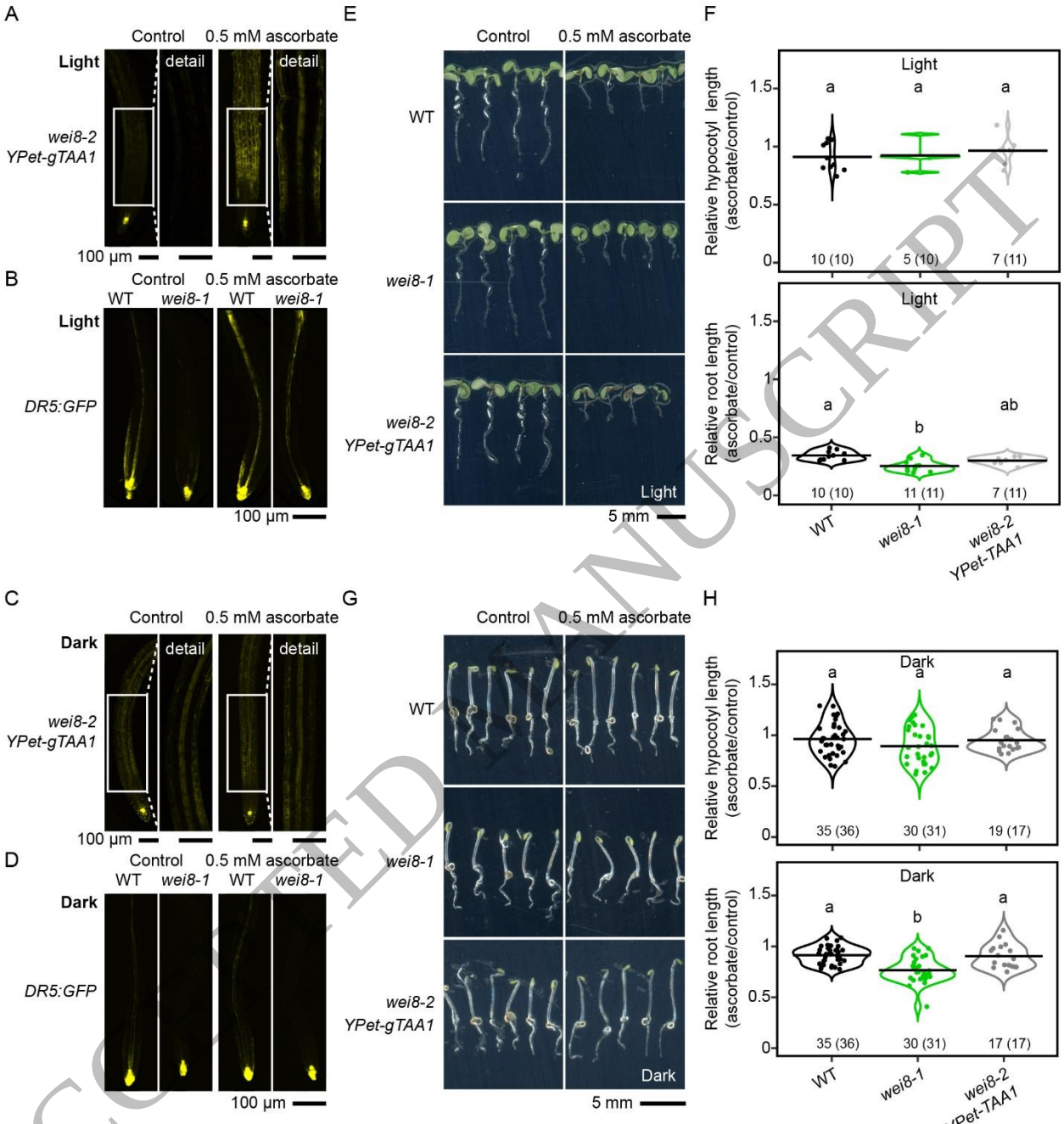

Figure 4
165x179 mm (x DPI)

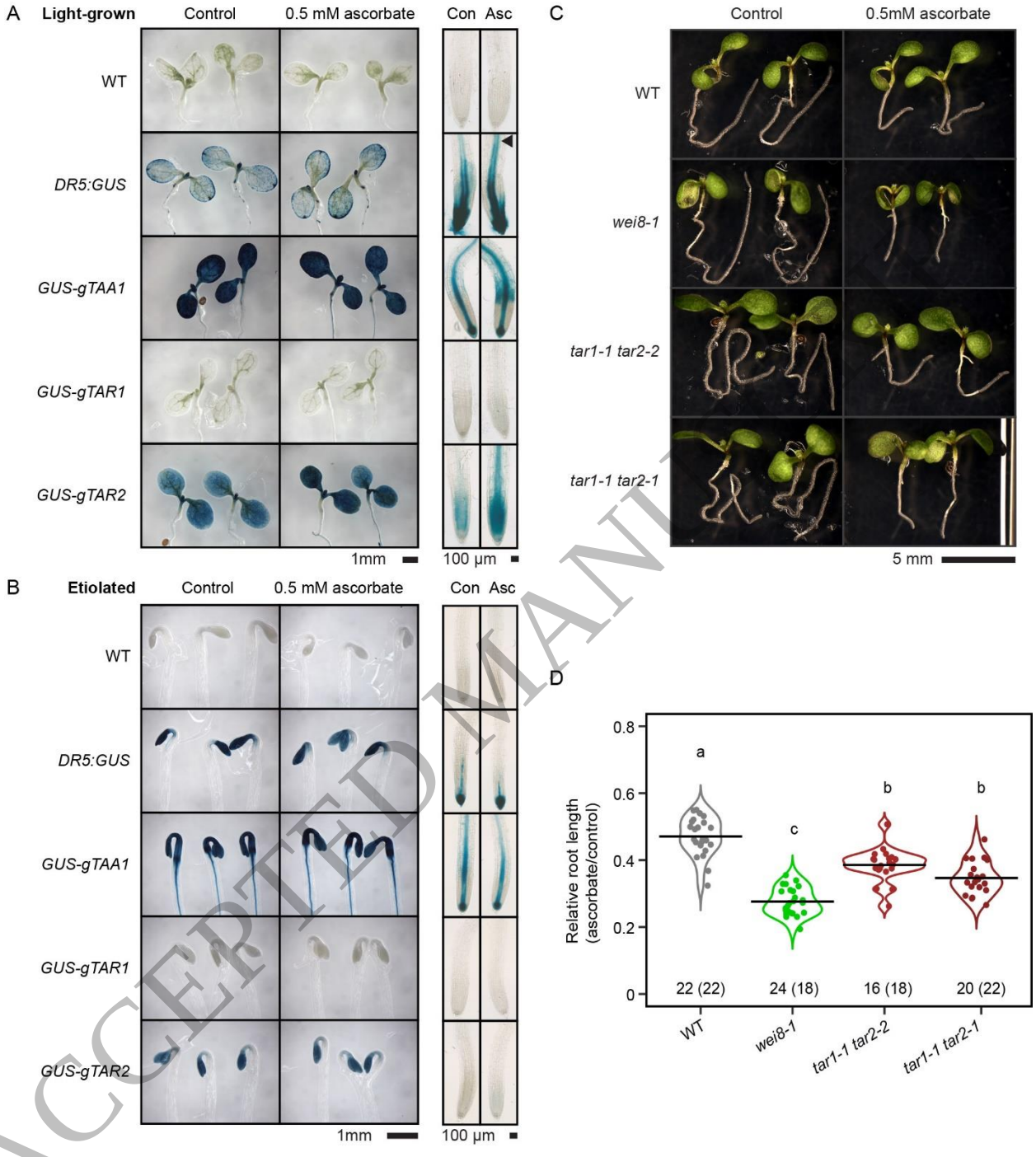

Figure 5
165x184 mm (x DPI)

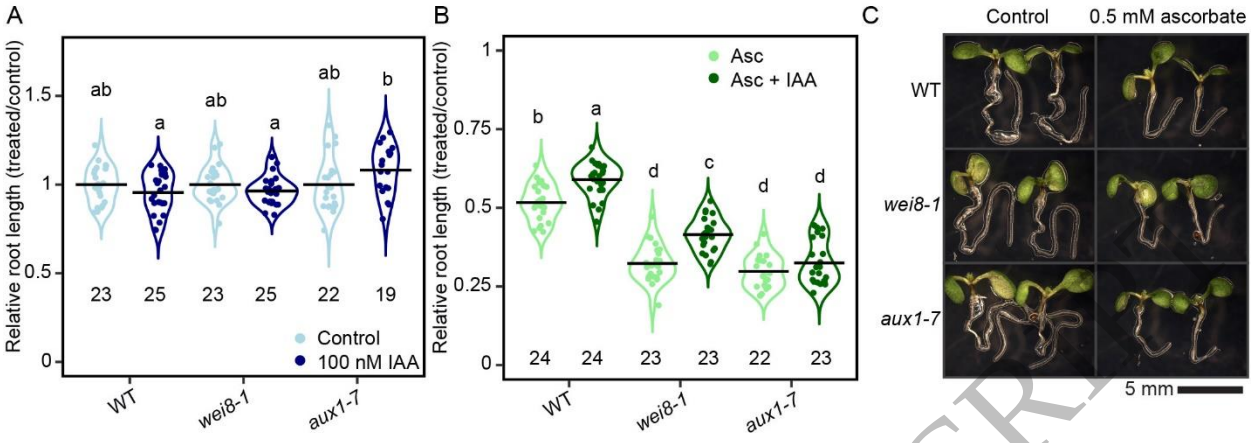

Figure 6
165x58 mm (x DPI)

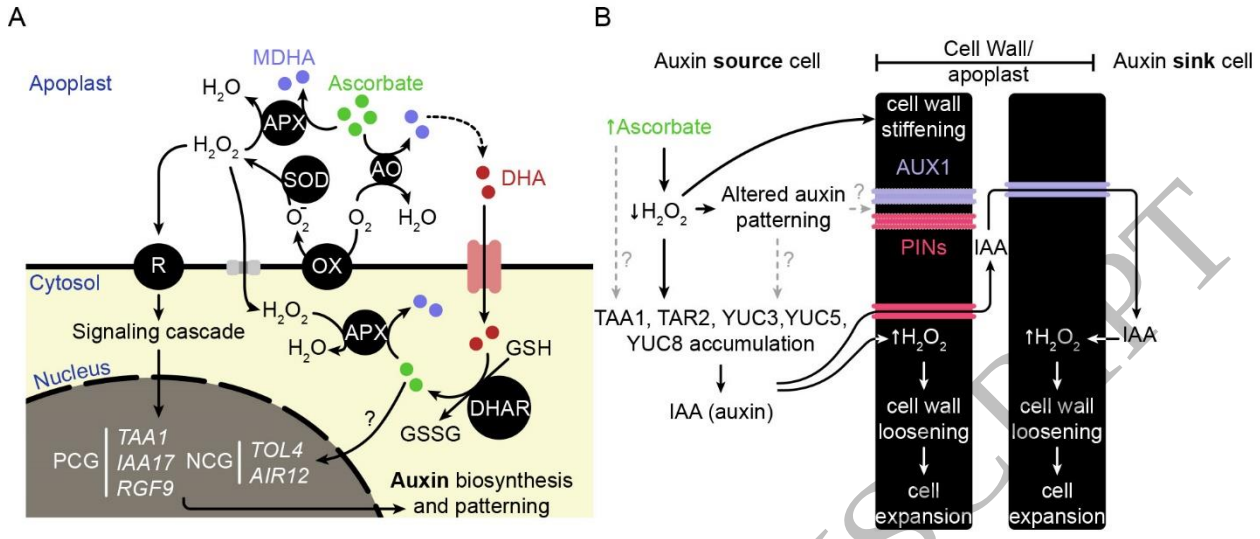

Figure 7
165x72 mm (x DPI)